commercial and recreational fisheries are composed of both populations of bluefin tuna (Fig. 2). A large fraction of the school (57.4%) and medium (44.3%) category bluefin tuna present in the U.S. waters of the Mid Atlantic Bight were from the eastern population, and we observed that the occurrence of eastern bluefin tuna in the Mid Atlantic Bight decreased with increasing size (age) (Fig. 3). Our estimates of trans-Atlantic exchange were significantly higher than previous reports from conventional tags (*3*) and demonstrated substantial intermingling of individuals from eastern and western populations in U.S. waters, a finding supported with recent evidence from electronic tags (*5*). In contrast, giant category bluefin tuna collected from northern U.S (Gulf of Maine) and Canadian (Gulf of St. Lawrence) fisheries were almost entirely of western origin (94.8% and 100%, respectively). The mechanism(s) responsible for differences in stock composition of bluefin tuna samples from Mid Atlantic Bight (mixed populations) and Gulf of Maine/Gulf of St. Lawrence (western population) waters appears related to size (age) or reproductive state. The majority of our sample from the Mid Atlantic Bight was composed of adolescent bluefin tuna (<5 years of age), and tagging studies have demonstrated that young bluefin tuna are more likely to display trans-Atlantic movements that are linked to foraging than are adults (*2*). Ontogenetic shifts in dispersive behaviors often occur for marine vertebrates displaying natal homing, with exploratory movements associated with foraging decreasing at the onset of breeding (*17*, *18*). Similarly, our finding of stock homogeneity of giants (>140 kg, >10 years of age) in the Gulf of Maine and Gulf of St. Lawrence, and increasing contributions from the western population with age in the Mid Atlantic Bight, suggests that movement becomes more limited and structured after bluefin tuna become sexually mature.

Significant trans-Atlantic mixing of eastern adolescents on western foraging areas emphasizes the connectivity of Atlantic bluefin tuna populations. Under the current assessment framework that assumes limited mixing, a high degree of exchange evident from chemical signatures in otoliths indicates that past abundances of western Atlantic bluefin tuna may have been overestimated, particularly at younger age classes. In addition, exchange rates reported here show that U.S. fisheries for bluefin tuna appear dependent, to some extent, on recruits from the Mediterranean Sea. Because the eastern population is at least an order of magnitude higher in abundance than the western population (*19*), it is unlikely that west-to-east movement of adolescents from the western population contribute significantly to Mediterranean and other eastern Atlantic fisheries. Of greater concern is that adolescents from the western population show similar eastward dispersive behaviors across the 45°W management boundary. If this occurs at rates observed here for eastern adolescents, the smaller, less productive western population will be disproportionately affected by higher fishing rates in the eastern management zone.

The disparity between the eastern and western population sizes and the continued decline of the western stock suggests that some added level of protection is needed to ensure the sustainability of the smaller western component. Natal homing rates reported here were remarkably high to both regions and clearly show that the contribution of eastern adults to the western spawning area is inconsequential. Thus, spawning adults in the Gulf of Mexico appear to be entirely of western origin, and this region should be given high priority for conservation. High connectivity between foraging areas in the Gulf of Maine/Gulf of St. Lawrence and the Gulf of Mexico was also observed, signifying that this region of the northern Atlantic represents critical refugia for western giants. Due to the condition of the western population, a more conservative rate of exploitation of bluefin tuna, inclusive of eliminating bycatch in the Gulf of Mexico, will be required for the recovery of this population.

References and Notes

1. D. Cushing, *Population Production and Regulation in the Sea* (Cambridge Univ. Press, Cambridge, 1995).
2. J. R. Rooker *et al.*, *Rev. Fish. Sci.* **15**, 265 (2007).
3. J. M. Fromentin, J. E. Powers, *Fish Fish.* **6**, 281 (2005).
4. A. Fonteneau, *Col. Vol. Sci. Pap. ICCAT* **60**, 1027 (2007).
5. B. A. Block *et al.*, *Nature* **434**, 1121 (2005).
6. G. R. Almany, M. L. Berumen, S. R. Thorrold, S. Planes, G. P. Jones, *Science* **316**, 742 (2007).
7. S. R. Thorrold, C. Latkoczy, P. K. Swart, *Science* **291**, 297 (2001).
8. Materials and methods are available as supporting material on *Science* Online.
9. S. R. Thorrold, S. E. Campana, C. M. Jones, P. K. Swart, *Geochim. Cosmochim. Acta* **61**, 2909 (1997).
10. A. N. LeGrande, G. A. Schmidt, *Geophys. Res. Lett.* **33**, L12604 (2006).
11. J. Ashford, C. Jones, *Geochim. Cosmochim. Acta* **71**, 87 (2007).
12. R. B. Millar, *Can. J. Fish. Aquat. Sci.* **44**, 583 (1987).
13. G. H. Rau, T. Takahashi, D. J. Des Marais, *Nature* **341**, 516 (1989).
14. S. L. H. Teo *et al.*, *Mar. Biol. (Berlin)* **151**, 1 (2007).
15. J. Carlsson, J. R. McDowell, J. E. L. Carlsson, J. E. Graves, *J. Hered.* **98**, 23 (2007).
16. T. P. Quinn, *Fish. Res.* **18**, 29 (1993).
17. J. R. Baker, G. A. Antonelis, C. W. Fowler, A. E. York, *Anim. Behav.* **50**, 237 (1995).
18. F. Maffucci, W. H. C. F. Kooistra, F. Bentiveyna, *Biol. Conserv.* **127**, 183 (2006).
19. J. J. Magnuson *et al.*, *An Assessment of Atlantic Bluefin Tuna* (National Academy Press, Washington, DC, 1994).

20. We thank S. Campana, J. Graves, and R. D. Wells for insightful comments on earlier versions of the manuscript. Special thanks to A. Belmonte, A. Boustany, B. Campbell, A. Corriero, M. DeFlorio, D. Dettman, J. Kaufman, M. Lutcavage, E. Rodriguez-Marin, P. Mace, E. Prince, N. Santamaria, G. Skomal, M. Stokesbury, S. Teo, P. Thompson, S. Turner, V. Tičina, R. Wingate, NOAA Observer Program, T.F.M. Tuna Farms of the Mediterraneo S.L., Tuna Graso, S.A., and Fish and Fish Ltd. for their assistance. Funding for this study was provided by NOAA (Southeast Fisheries Science Center and Saltonstall-Kennedy Program), the International Fisheries Governance Program of Fisheries and Oceans Canada, Monterey Bay Aquarium, Tag-A-Giant Foundation, and the Large Pelagic Research Center (University of New Hampshire).

Supporting Online Material

www.sciencemag.org/cgi/content/full/1161473/DC1
Materials and Methods
Fig. S1
References
SOM Data

6 June 2008; accepted 17 September 2008
Published online 2 October 2008;
10.1126/science.1161473
Include this information when citing this paper.

Glia Are Essential for Sensory Organ Function in *C. elegans*

Taulant Bacaj,* Maya Tevlin,* Yun Lu, Shai Shaham†

Sensory organs are composed of neurons, which convert environmental stimuli to electrical signals, and glia-like cells, whose functions are not well understood. To decipher glial roles in sensory organs, we ablated the sheath glial cell of the major sensory organ of *Caenorhabditis elegans*. We found that glia-ablated animals exhibit profound sensory deficits and that glia provide activities that affect neuronal morphology, behavior generation, and neuronal uptake of lipophilic dyes. To understand the molecular bases of these activities, we identified 298 genes whose messenger RNAs are glia-enriched. One gene, *fig-1*, encodes a labile protein with conserved thrombospondin TSP1 domains. FIG-1 protein functions extracellularly, is essential for neuronal dye uptake, and also affects behavior. Our results suggest that glia are required for multiple aspects of sensory organ function.

Glia, the largest cell population in vertebrate nervous systems, are implicated in processes governing nervous system development and function (*1*). However, the functions of few glial proteins are characterized. Astrocytic glia are often positioned near synapses and can respond to and participate in synaptic activity (*2*, *3*), influencing the response of postsynaptic cells to presynaptic stimulation (*4*).

Sensory neurons convert environmental stimuli into neuronal activity, and their receptive endings are often associated with glia, such as retinal pig-

Laboratory of Developmental Genetics, The Rockefeller University, 1230 York Avenue, New York, NY 10065, USA.

*These authors contributed equally.
†To whom correspondence should be addressed. E-mail: shaham@rockefeller.edu

mented epithelial cells and Müller glia or olfactory ensheathing cells. Because sensory neurons are postsynaptic to the environment, their associated glia may affect sensory activity in ways analogous to synaptic astrocytes.

Sensory organs are conserved structures, exhibiting morphological, functional, and molecular similarities among diverged species (*5*). To understand glial contributions to sensory neuron functions, we studied the largest sensory organ of the nematode *Caenorhabditis elegans*, the amphid. This organ mediates responses to chemical, thermal, and tactile stimuli, promoting attractive and repulsive behaviors that are easily assayed. Each of the bilateral amphids comprises 12 neurons extending ciliated dendrites to the anterior tip (*5*). These neurons can be grouped based on association with the single amphid sheath glial cell: The dendritic receptive endings of four neurons are entirely surrounded by this glial cell in a hand-in-glove configuration, whereas remaining cilia are encased in a channel formed by the same glial cell and are exposed, through a pore, to the outside environment (*5*, *6*) (fig. S1).

We ablated sheath glia in first-stage larvae, after the amphid had formed, by either using a laser microbeam (*7*) or expressing the diphtheria toxin A gene from a sheath-glia–specific promoter (*8*). Ablation success was monitored by disappearance of a glia-specific green fluorescent protein (GFP) reporter, and by electron microscopy (EM) reconstruction of amphid sensory endings. We first examined the glia-embedded sensory neurons AWC, AWA, and AWB. Animals with bilateral sheath-glia ablation display severe defects in AWC-mediated chemotaxis toward benzaldehyde or isoamyl alcohol (*9*) (Fig. 1A), behaving comparably to *che-2(e1033)* mutants, which lack functional sensory cilia (*10*). Similarly, ablation also reduced chemotaxis toward AWA-sensed odorants (Fig. 1C). By contrast, AWB function was not affected by sheath glia ablation (Fig. 1E).

To confirm these neuron-selective effects of glia on odortaxis, we expressed the ODR-10 diacetyl receptor, normally found only in AWA (*11*), also in AWB neurons. As previously described (*12*), animals expressing ODR-10 in both neurons are less attracted to diacetyl than wild-type animals, reflecting the opposing behavioral outputs of these neurons (Fig. 1G). However, consistent with a defect in AWA, sheath-glia ablated animals expressing ODR-10 in both neurons are repelled by diacetyl (Fig. 1G). In glia-ablated animals, the extracellular environment of AWA and AWB is identical. The normal AWB response, therefore, suggests that odorant molecules can access and interact with odorant receptors in the absence of glia and that the presence of glia is required for integrating opposing environmental stimuli.

We also examined thermotaxis, a behavior mediated by the AFD sheath-glia embedded neuron. Whereas wild-type animals seek their cultivation temperature on a thermal gradient (*13*, *14*), inactivation of AFD by cell ablation or by the *ttx-1*(*p767*) mutation results in cryophilic/athermotactic behavior (*14*). Sheath-glia ablation does not seem to eliminate AFD function but results in thermophilic behavior (fig. S2), suppressible by *ttx-1*(*p767*) (fig. S2D).

The ciliated sensory receptive endings of AWC, AWA, AFD, and to a lesser extent AWB, were defective in sheath-glia ablated animals (Fig. 1). Sheath-glia ablation resulted in complete loss of the AWC wing-like cilium structure (Fig. 1B) (n >100), and expansion of this structure in dauer animals was also blocked (fig. S3) (n = 2). Similarly, the highly branched processes of the AWA cilium were largely eliminated in sheath-glia ablated animals (Fig. 1D) (n = 10), as were the microvilli-like extensions of the AFD sensory ending (Fig. 1H) (n = 15). Ciliary localization of olfactory signaling proteins, including ODR-10 (AWB, Fig. 1F; AWA,

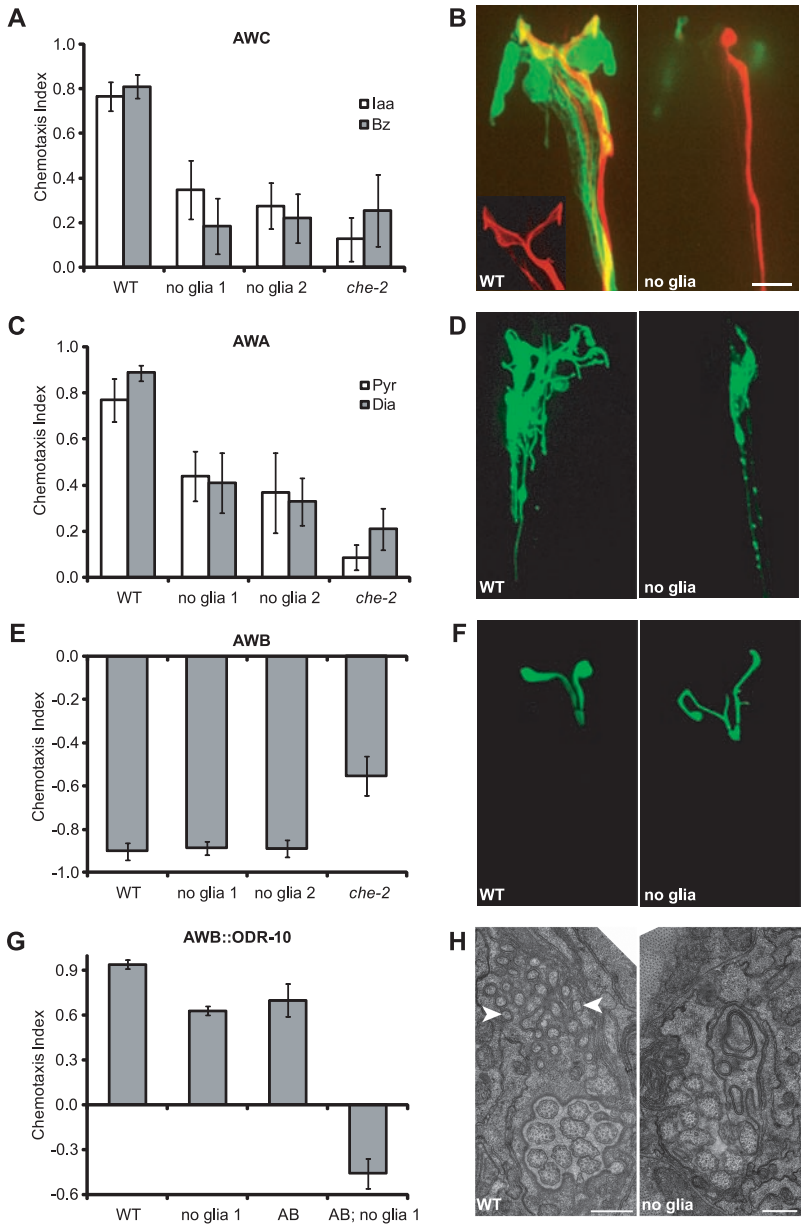

Fig. 1. Glia are required for behavior and cilium structure. (**A**) Glia-ablated animals have defective AWC-mediated odortaxis toward 1% isoamyl alcohol (Iaa) and 0.5% benzahldehyde (Bz), $P < 0.001$ (Student's t test). (**B**) A wild-type AWC cilium (red, *odr-1*::RFP) ensheathed by an amphid sheath glia (green, *vap-1*::GFP). Glia ablation in the contralateral amphid results in an amorphous cilium. Anterior, up. Scale bar, 5 μm. (**C**) Glia-ablated animals have defective AWA-mediated odortaxis toward 1% methyl pyrazine (Pyr) and 0.1% diacetyl (Dia), $P < 0.001$. (**D**) Glia removal decreases AWA cilium branching (*odr-3*::ODR-3p::GFP). (**E**) Glia are not required for AWB function, 10% 2-nonanone avoidance. (**F**) AWB cilium morphology appears grossly normal, although additional branching and failure of the two cilia to spread is often observed (*str-1*::ODR-10::GFP). (**G**) Animals expressing ODR-10 in AWA and AWB (AB) are attracted to diacetyl. However, dual-sensing animals lacking glia are repelled. (**H**) EM showing absence of AFD microvilli-like projections (arrowheads) in glia-ablated animals. Scale bar, 0.5 μm. WT, wild type; no glia, diphtheria-toxin-ablated glia; *che-2, che-2(e1033)* mutants; error bars, SD of 12 or more assays.

AWC, fig. S4), the G-alpha protein ODR-3 (AWA, Fig. 1D), and the cyclic-nucleotide-gated channel subunit TAX-4 (AWC, fig. S4), was unaltered.

We next examined behaviors mediated by amphid channel neurons. Sheath-glia ablation completely blocked chemotaxis toward NaCl (Fig. 2A), a behavior mediated by the ASE neurons (*15*). Avoidance of a high osmolarity barrier, mediated by ASH (*16*), was also entirely abrogated (Fig. 2B), as was long-range avoidance of 1-octanol (Fig. 2C), a behavior mediated in part by ADL (*12*). Surprisingly, sensory ending morphology, length, and microtubule organization of all channel neurons appeared normal in ablated animals (Fig. 2, D and E, and fig. S1). Furthermore, ciliary localization of intraflagellar transport components (CHE-11, DYF-11), or of ODR-10, expressed in ASH, was not disrupted by sheath-glia ablation (fig. S4).

We used G-CaMP to examine Ca^{2+} level changes in ASH in response to high osmolarity. Whereas wild-type animals increase intracellular Ca^{2+} after exposure to and removal of an osmotic stimulus (Fig. 3A and fig. S5) (*17*), sheath-glia ablated animals lacked these responses (Fig. 3B and fig. S5). To determine whether signaling downstream of Ca^{2+} elevation was disrupted, we expressed the light-activated channel channelrhodopsin-2 (ChR2) (*18*) within ASH. In the presence of retinal, a ChR2 cofactor, glia-ablated (and wild-type) animals initiate backward locomotion (Fig. 3C), demonstrating that downstream signaling is intact and that glia are not required for ASH health/viability.

When *C. elegans* are soaked in lipophilic dyes (e.g., DiI), some channel neurons, and AWB, take up and concentrate the dye. DiI uptake was eliminated in all amphid neurons in glia-ablated animals (Fig. 2F). Thus, dye filling (defective in channel neurons and AWB), ciliary morphology (defective mainly in AWA, AWC, and AFD), and behavior generation (not defective in AWB) are independent properties of amphid sensory neurons, each requiring the presence of sheath glia.

To uncover glial factors controlling these neuronal properties, we compiled a list of amphid sheath-glia–enriched transcripts. mRNA from cultured GFP-expressing amphid-sheath glia was compared to mRNA from other cultured embryonic cells by hybridizing each population to an oligonucleotide gene array. We identified 298 unique transcripts with greater than fourfold enrichment (table S1), including the known glial genes *daf-6* and *vap-1* (*19*). Of 298 transcripts, 159 are predicted to encode transmembrane or secreted proteins that could potentially interact with amphid sensory neurons. These secreted proteins include Ca^{2+} binding proteins and a KCl cotransporter, which may explain glial contributions to Ca^{2+} elevation in ASH.

To validate our results, we generated GFP reporter fusion constructs to promoters of seven genes. Five were expressed exclusively in amphid sheath glia and phasmid sheath glia (an amphid-like tail sensory organ) (Fig. 4, A and B, and fig. S6).

We screened enriched genes by RNA interference (RNAi) for defects in amphid neuron dye filling (Dyf phenotype) and identified the gene F53B7.5, which we renamed *fig-1* (Dyf, expressed in glia). RNAi against *fig-1* resulted in dye-filling defects in amphids and phasmids (Fig.

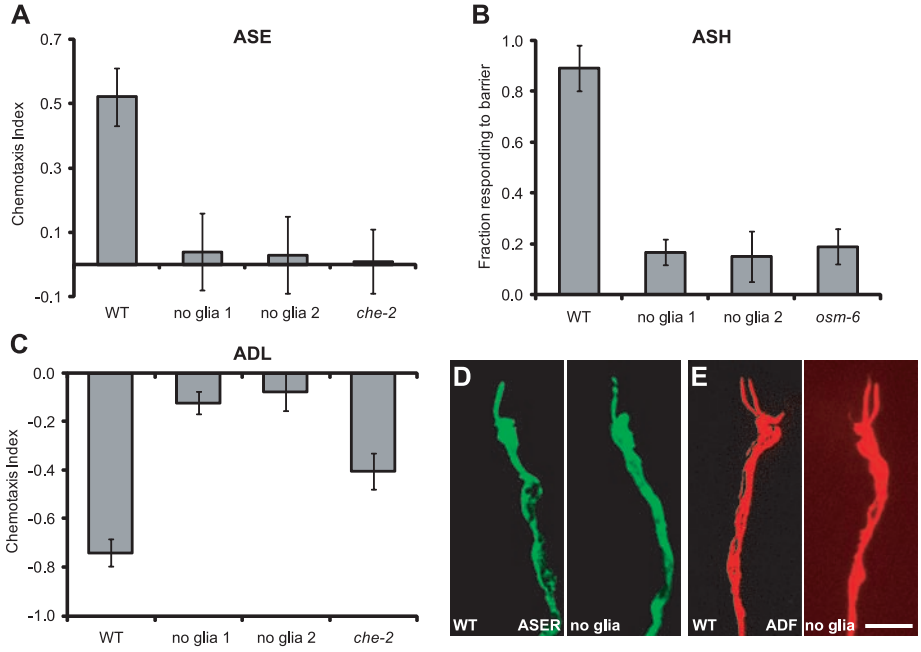

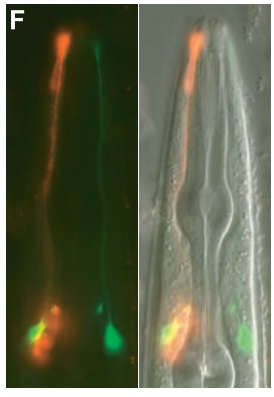

Fig. 2. Glia affect channel neuron function but not morphology. (**A**) Glia-ablated animals fail to detect 0.2 M NaCl ($P < 0.001$), an ASE-mediated behavior. (**B**) Glia-ablated animals fail to avoid a 4 M fructose ring ($P < 0.001$), an ASH-mediated behavior. *osm-6*, *osm-6(p811)* mutants. (**C**) Glia-ablated animals fail to avoid 1-octanol in a long-range assay ($P < 0.001$), a behavior partially mediated by ADL. (**D** and **E**) The morphology of amphid channel neurons is not affected by glia removal. ASER, *gcy-5*::GFP; ADF, T08G3.3::RFP). Scale bar, 5 μm. (**F**) Glia are required for neuronal uptake of DiI (red). Only the right amphid sheath glia is ablated. AWC (green, *odr-1*::YFP) indicates the location of the dendrite bundles. Error bars, SD of 12 or more assays.

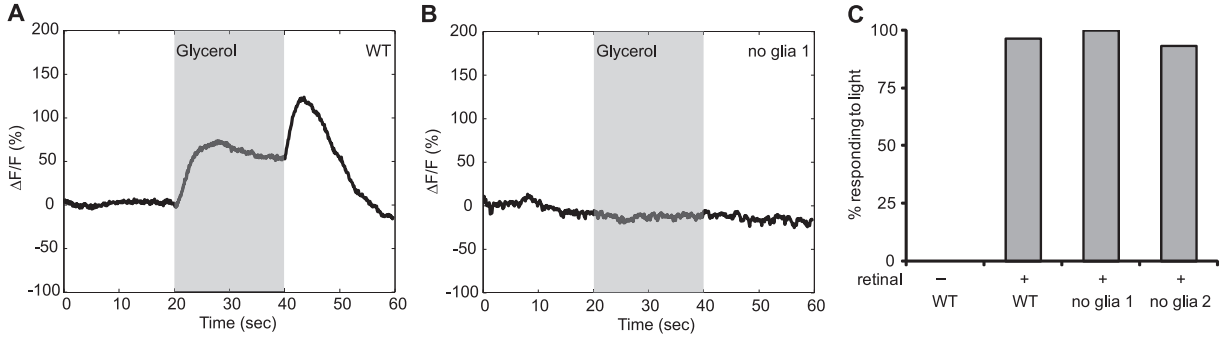

Fig. 3. Glia are required for Ca^{2+} responses in ASH. (**A**) As determined by G-CaMP fluorescence, ASH responds to application and removal of 1M glycerol (*17*). Shaded region, stimulus duration. (**B**) ASH fails to respond to glycerol in glia-ablated animals. (**C**) Glia are not required for neuronal function downstream of Ca^{2+} entry. Activation of ASH-expressed ChR2 by light causes animals to move backward; $n = 30$ for each.

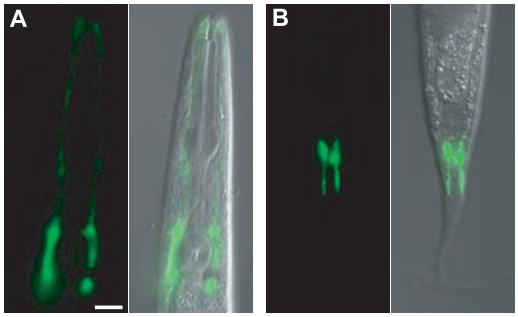

C

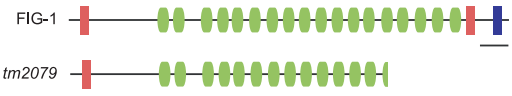

D

Genotype	Normal Dye Filling (%) Amphid	Phasmid
WT	100	100
fig-1 (RNAi)	60	30
fig-1(tm2079)	18	0
fig-1(tm2079); C38G2	90	100
fig-1(tm2079); $P_{fig\text{-}1}$ *fig-1* (long)	50	44
fig-1(tm2079); $P_{fig\text{-}1}$ *fig-1* (short)	46	42
fig-1(tm2079); P_{glia} *fig-1*	60	15
fig-1(tm2079); P_{neuron} *fig-1*	80	0

E

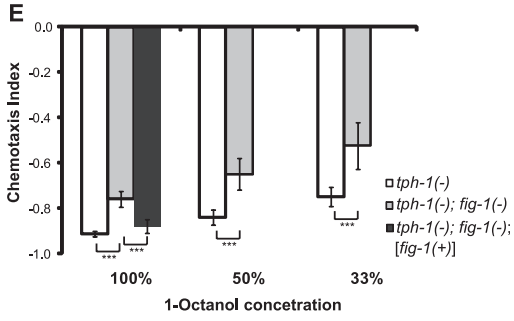

Fig. 4. Glial *fig-1* is required for neuronal dye filling and function. (**A** and **B**) *fig-1* is expressed in amphid (**A**) and phasmid (**B**) sheath glia. Anterior, up. Scale bar, 5 μm. (**C**) FIG-1 domain structure. Red, thrombospondin type 1 domain; green, C6 repeats; blue, EGF-like type II domain; bar, 200 amino acids. The predicted protein in the *fig-1(tm2079)* deletion is shown. (**D**) *fig-1* is required for DiI accumulation. One representative line shown for each condition: C38G2, cosmid containing *fig-1*; glial promoter, T02B11.3; neuronal promoter, *sra-6*; $n > 40$ for each. (**E**) *fig-1* is required for 1-octanol avoidance. Assays were performed in the *tph-1(mg280)* background, which suppresses movement defects of *fig-1(tm2079)* animals. *fig-1(tm2079)* mutants perform worse at all three concentrations, and these defects can be rescued by *fig-1(+)*. Asterisks, $P < 0.001$. Error bars, 95% confidence intervals. At least 24 assays for each condition.

4D). An 1117-bp deletion in *fig-1*, *tm2079*, also perturbed dye filling (Fig. 4C), and this defect was rescued by a cosmid spanning the *fig-1* locus. Interestingly, *fig-1(tm2079)* mutants exhibited normal neuronal and amphid sheath glia structure (fig. S1I), demonstrating that access to dye is not sufficient for dye filling and that glia-dependent neuronal properties are required for dye filling.

fig-1(RNAi) defects could be induced at all developmental stages and were observed within 24 hours of double-stranded RNA exposure (table S2), suggesting that although *fig-1* mRNA is highly expressed (table S1), FIG-1 protein must be labile, consistent with a nonstructural role.

Expression of a *fig-1* promoter::GFP reporter was detected exclusively within amphid and phasmid sheath glia (Fig. 4, A and B) and was first evident in late embryos, continuing throughout adulthood. Thus, FIG-1 expression may be required continuously for neuronal dye filling.

fig-1 is predicted to generate two alternatively spliced mRNAs encoding proteins of 3095 (long) and 2892 (short) amino acids, the short isoform being sufficient for rescue (Fig. 4D). Both proteins contain an N-terminal signal sequence, a TSP1 thrombospondin domain, 18 C6 domains, and a second TSP1 domain (Fig. 4C). The larger protein is also predicted to contain an EGF-like type II motif at its C terminus (*8*). TSP1 and EGF-like motifs are characteristic domains found in astrocyte-secreted thrombospondin proteins implicated in synapse development (*20*).

To determine whether FIG-1 protein can act cell nonautonomously, we expressed a *fig-1*(short) cDNA transgene under either sheath glia (T02B11.3) or sensory neuron (*sra-6*; ASH, and weakly in ASI, PHA, and PHB) promoters. Both transgenes rescued *fig-1*(*tm2079*) mutants (Fig. 4D), as expected if FIG-1 acted extracellularly.

Finally, although *fig-1*(*tm2079*) mutants exhibited normal behavior toward most stimuli tested (fig. S7), we identified a modest but significant defect in 1-octanol avoidance (Fig. 4E), suggesting that *fig-1* also contributes to behavior generation.

We have demonstrated that *C. elegans* amphid sheath glia provide associated neurons with at least three separate activities and have identified a molecular mediator contributing to two of these functions. Recent studies suggest that *C. elegans* glia share developmental similarities with vertebrate glia (*21*). At least some of the glial functions we describe might, therefore, be conserved in other sensory systems.

Astrocyte-secreted thrombospondins play important postsynaptic roles in synapse assembly and function (*20*). Our studies of FIG-1, which contains domains also present in thrombospondins, demonstrate that this glial factor plays a key role in modulating sensory neuron properties. The rapid turnover of FIG-1 protein is intriguing, suggesting possible dynamic roles. Could FIG-1 and thrombospondins have related molecular functions? Sensory receptive endings share some similarities with postsynaptic neuronal endings. Both respond to diffusible cues by activating G protein–coupled receptors (*11*) or ligand-gated ion channels (*22*); postsynaptic dendritic spines are highly malleable in shape and size (*23*, *24*), as are sensory neuron receptive endings (*25*); and many vertebrate excitatory synapses are ensheathed by glia, as are sensory neuron receptive endings. These observations, together with the domain structure of FIG-1, suggest the highly speculative notion that analogies between the "sensory synapse" and true synapses might, in part, reflect molecular homologies. Our results provide strong evidence for essential glial contributions to sensory organ function.

References and Notes

1. P. G. Haydon, *Nat. Rev. Neurosci.* **2**, 185 (2001).
2. G. Perea, A. Araque, *Science* **317**, 1083 (2007).
3. G. Perea, A. Araque, *J. Neurosci.* **25**, 2192 (2005).
4. R. Robitaille, *Neuron* **21**, 847 (1998).
5. S. Ward, N. Thomson, J. G. White, S. Brenner, *J. Comp. Neurol.* **160**, 313 (1975).
6. L. A. Perkins, E. M. Hedgecock, J. N. Thomson, J. G. Culotti, *Dev. Biol.* **117**, 456 (1986).
7. C. I. Bargmann, L. Avery, *Methods Cell Biol.* **48**, 225 (1995).
8. Materials and methods are available as supporting material on *Science* Online.
9. C. I. Bargmann, E. Hartwieg, H. R. Horvitz, *Cell* **74**, 515 (1993).
10. M. Fujiwara, T. Ishihara, I. Katsura, *Development* **126**, 4839 (1999).
11. P. Sengupta, J. H. Chou, C. I. Bargmann, *Cell* **84**, 899 (1996).
12. E. R. Troemel, B. E. Kimmel, C. I. Bargmann, *Cell* **91**, 161 (1997).
13. E. M. Hedgecock, R. L. Russell, *Proc. Natl. Acad. Sci. U.S.A.* **72**, 4061 (1975).
14. I. Mori, Y. Ohshima, *Nature* **376**, 344 (1995).
15. C. I. Bargmann, H. R. Horvitz, *Neuron* **7**, 729 (1991).
16. C. I. Bargmann, J. H. Thomas, H. R. Horvitz, *Cold Spring Harb. Symp. Quant. Biol.* **55**, 529 (1990).
17. M. A. Hilliard *et al.*, *EMBO J.* **24**, 63 (2005).
18. G. Nagel *et al.*, *Proc. Natl. Acad. Sci. U.S.A.* **100**, 13940 (2003).
19. E. A. Perens, S. Shaham, *Dev. Cell* **8**, 893 (2005).
20. K. S. Christopherson *et al.*, *Cell* **120**, 421 (2005).
21. S. Yoshimura, J. I. Murray, Y. Lu, R. H. Waterston, S. Shaham, *Development* **135**, 2263 (2008).
22. K. Sato, M. Pellegrino, T. Nakagawa, L. B. Vosshall, K. Touhara, *Nature* **452**, 1002 (2008).
23. J. T. Trachtenberg *et al.*, *Nature* **420**, 788 (2002).
24. K. K. Murai, L. N. Nguyen, F. Irie, Y. Yamaguchi, E. B. Pasquale, *Nat. Neurosci.* **6**, 153 (2003).
25. S. Mukhopadhyay, Y. Lu, S. Shaham, P. Sengupta, *Dev. Cell* **14**, 762 (2008).

26. We thank C. Bargmann and S. Chalasani for their generous help with G-CaMP imaging, N. Pokala for the ASH-ChR2 strain and advice on assays, H. Fares for a DT-A plasmid, S. Mazel for help with fluorescence-activated cell sorting, S. Mitani for the *tm2079* allele, A. North for help with microscopy, E. Nudleman for the thermotaxis apparatus, Shaham laboratory members for comments on the project and manuscript, and C. Bargmann, P. Sengupta, O. Hobert, and E. Jorgensen for strains. S.S. is a Klingenstein Fellow in the Neurosciences.

Supporting Online Material

www.sciencemag.org/cgi/content/full/322/5902/744/DC1
Materials and Methods
Figs S1 to S7
Table S1 and S2
References

10 July 2008; accepted 18 September 2008
10.1126/science.1163074

Supporting Online Material for

Glia Are Essential for Sensory Organ Function in *C. elegans*

Taulant Bacaj, Maya Tevlin, Yun Lu, Shai Shaham*

*To whom correspondence should be addressed. E-mail: shaham@rockefeller.edu

Published 31 October 2008, *Science* **322**, 744 (2008)
DOI: 10.1126/science.1163074

This PDF file includes:

Supporting Online Material for

Glia Are Essential for Sensory Organ Function in *C. elegans*

Taulant Bacaj*, Maya Tevlin*, Yun Lu, Shai Shaham†

*These authors contributed equally.

†To whom correspondence should be addressed. E-mail: shaham@rockefeller.edu

This PDF file includes:

Supporting Online Material

Materials and Methods

Strains

C. elegans strains were cultured at 20°C as described (*1*), unless otherwise indicated. Wild-type animals were Bristol strain N2. Other alleles used in this work were: LGV: *ttx-1*(*p767*), *osm-6(p811)*, *fig-1(tm2079)*; LGX: *che-2(e1033)*. The following transgenic arrays were used:

"no glia 1" *nsIs109* [F16F9.3 pro::DT-A(G53E) + *unc-122* pro::GFP],
"no glia 2" *nsIs113* [F16F9.3 pro::DT-A(G53E) + *unc-122* pro::GFP] X,
cbIs1 [*vap-1* pro::nlsGFP + *lin-15*(+)] I,
kyIs90 [*odr-3* pro::*odr-3*(1st 35 aa's)::GFP + *lin-15*(+)] III,
ntIs1 [*gcy-5* pro::GFP + *lin-15*(+)] V,
oyIs17 [*gcy-8* pro::GFP + *lin-15*(+)] V,
oyIs45 [*odr-1* pro::RFP] V,
kyIs156 [*str-1* pro::*odr-10*::GFP] X,
oyIs51 [T08G3.3 pro::RFP],
kyEx728 [*sra-6* pro::G-CaMP],
kyEx1440 [*sra-6* pro::*chop2*::Cherry + *elt-2* pro::GFP],
kyEx1449 [*sra-6* pro::*chop2*::Cherry + *elt-2* pro::GFP],
myEx10 [*che-11* pro::*che-11*::GFP, *rol-6(su1006)*],
nsEx1705 [*dyf-11* pro::*dyf-11*::GFP, *rol-6(su1006)*],
nsEx856 [F16F9.3 pro::GFP, *rol-6(su1006)*],
nsEx864 [F11C7.2 pro::GFP, *rol-6(su1006)*],
nsEx1066 [F53F4.13 pro::GFP, *rol-6(su1006)*],
nsEx1086 [T02B11.3 pro::GFP, *rol-6(su1006)*],
nsEx1758 [*fig-1* pro::GFP, *rol-6(su1006)*],
nsEx2192 [C38G2, *rol-6(su1006)*],
nsEx2209 [*fig-1* pro::*fig-1* (long), *exp-1* pro::GFP],
nsIs184 [*fig-1* pro::*fig-1* (short), *exp-1* pro::GFP],
nsEx2155 [T02B11.3 pro::*fig-1* (short), *exp-1* pro::GFP],
nsEx2150 [*sra-6* pro::*fig-1* (short), *exp-1* pro::GFP],
nsEx2212 [*sra-6* pro::*odr-10*::GFP, *rol-6(su1006)*, pSL1180],
nsEx2215 [*odr-1* pro::*odr-10*::GFP, *rol-6(su1006)*, pSL1180],
nsEx2218 [*odr-10* pro::*odr-10*::GFP, *rol-6(su1006)*, pSL1180],
nsEx2221 [*odr-1* pro::*tax-4*::GFP, *rol-6(su1006)*, pSL1180],
nsEx2224 [*odr-1* pro::*tax-4*::GFP, *rol-6(su1006)*, pSL1180].

P_{exp-1}GFP was kindly provided by Eric Jorgensen (*2*), pSL1180 is an empty cloning vector used to increase the DNA concentration of injection mixtures. Germline transformations were performed as described (*3*). Stable transgenes were obtained via psoralen integration (*4*).

Ablations

Laser ablations were performed as described (*5*) in L1 larvae of a strain expressing GFP in amphid sheath glia (*cbIs1*). Ablation success was determined by lack of GFP expression and also confirmed in eight animals by EM reconstruction. All cilia morphologies were determined in laser ablated animals as well as transgenic lines lacking glia. An attenuated form of diphtheria toxin A was expressed specifically within amphid and phasmid sheath cells using the F16F9.3 promoter region to kill these cells genetically. Transgenic animals carrying pTB29 [F16F9.3 pro::DT-A(G53E)], injected at 2 ng/μL, and pEP51 [*unc-122* pro::GFP], a gift of Elliot Perens, were obtained by germline injection followed by psoralen integration. In the two lines characterized, "no glia 1" (*nsIs109*) and "no glia 2" (*nsIs113*), the amphid sheath glia appear to die in late embryos or in early L1 larvae. Laser-ablated animals were tested in NaCl chemotaxis and osmosensation assays and they performed similarly to genetically-ablated animals, indicating that the two ablations are essentially equivalent.

Behavioral analysis

NaCl chemotaxis and odortaxis assays were performed as previously described (*6*, *7*). Attractants were assayed on circular plates; repellents and diacetyl in the experiment shown in Fig. 1G were assayed on square plates. All data shown is from 12 assays. The ring assay was used to test osmosensation (*8*). Briefly, a 1-cm ring of 4 M fructose containing the dye Congo Red was made on an NGM plate. Animals were placed inside the ring and followed over the next 10 min to determine the response to the osmotic barrier. Animals avoiding the ring more than six times were classified as normal; those exiting the ring in less than six attempts were deemed defective in osmosensation.

Thermotaxis assays were performed on a 18°-26°C linear temperature gradient (*9*). Animals were allowed to lay for 8-24 hours and removed from plates. The staged progeny were tested on the first day of adulthood. Briefly, animals were washed twice with S-Basal and spotted onto a 10-cm plate containing 12 mL of NGM agar. The plate was placed onto the temperature gradient with the addition of 1 mL glycerol to its bottom to improve thermal conductivity. The plate was covered with a flat piece of glass. The assay was stopped after 45 min by inverting the plate over chloroform thus killing the animals. The plates have an imprinted 6x6 square pattern which formed the basis of the 6 temperature bins. The data shown is the average of four assays.

Dye filling

Stock solutions (5 mg/mL) of 1,1'-dioctadecyl-3,3,3',3'-tetramethylindocarbocyanine perchlorate (DiI) in *N*,*N*-dimethylformamide were stored at -20°C. To assay dye uptake, animals were soaked in 5 μg/mL DiI diluted in M9 for 20-60 min.

Microscopy and Imaging

GFP expression patterns were analyzed in stable transgenic lines by conventional fluorescence microscopy using an Axioplan II microscope equipped with an AxioCam camera. Alternatively, imaging was performed on a Zeiss Axiovert 200M microscope equipped with an UltraView spinning disk confocal head using a 100x/1.45 NA objective.

Calcium imaging was performed using a microfluidic device as described (*10*). Images were captured at 10 frames/sec and were analyzed using MetaMorph and Matlab (*10*).

Electron Microscopy

Animals were fixed, stained, embedded in resin, and serially sectioned using standard methods (*11*). Imaging was performed with a transmission electron microscope equipped with a digital camera.

Channelrhodopsin2

An overnight culture (5mL) of *E. coli* (strain OP50) was pelleted and concentrated to 50 µL. To this, 1 µL of 50 mM retinal (a gift of Navin Pokala and Cori Bargmann) was added. After vortexing, the mixture was spotted in NGM plates. Animals expressing ChR2-mCherry were transferred and cultivated on these plates for at least 2 hours. Animals were assayed on a dissecting microscope by exposing them for about 1 second to excitation light using a GFP Plant fluorescence filter 470/40nm. Animals initiating backward movement within 2 seconds were scored responsive. The animals were not responding to UV light per se as omission of retinal, a channelrhodopsin2 obligate cofactor, resulted in unresponsive animals.

Cell Culture

Embryonic cells were obtained using methods previously described (*12*, *13*). Briefly, embryos were isolated from gravid adults following lysis in a hypochlorite solution. Eggs released by this treatment were pelleted by centrifugation and washed with sterile egg buffer containing 118 mM NaCl, 48 mM KCl, 2 mM $CaCl_2$, 2 mM $MgCl_2$, and 25 mM HEPES (pH 7.3). Eggshells were removed by incubation in 5 ml chitinase (0.5 U/ml in egg buffer) for 45 minutes. Embryos were pelleted by brief centrifugation, and the egg buffer was removed and replaced with 2 ml L-15 medium supplemented with 10% FBS, 50 U/ml penicillin and 50 µg/ml streptomycin. The osmolarity of the culture medium was adjusted to 340 mOsm with sucrose.

The embryos were dissociated by passage through a 5µm syringe filter. Cells were plated on poly-L-lysine (0.01%) coated cell culture dishes at a density of 10^7 cells/ml and maintained in L-15 media at 22°C in a humidified chamber. The cells were cultured for 24 hr to allow differentiation of GFP-labeled amphid sheath cells. The *vap-1::GFP* transgene used also drives faint expression in the AFD neuron.

FACS analysis

Sorting experiments were performed on a FACSVantage SE/DiVa, equipped with a 488 nm laser. The machine was flushed with egg buffer prior to sorting to enhance cell

viability. Autofluorescence levels were established by flow cytometry of cells isolated from the non-GFP-expressing wild-type strain (N2). The sorting gate for size and granularity was empirically adjusted to exclude cell clumps and debris and to achieve ~95% enrichment for GFP-labeled cells, which represented 0.1% of the total cell count. The cells were collected directly into RNA extraction buffer. As a reference, equal amounts of non-GFP cells were collected by FACS for RNA isolation.

Isolation and amplification of RNA

For each experiment, mRNA was isolated from 90,000 - 120,000 cells using the Absolutely RNA microprep kit. 90-150 ng of obtained total RNA was subjected to linear amplification, fragmentation and biotin labeling using the Ovation™ Biotin RNA Amplification and Labeling System as recommended by the manufacturer. The quality and size distribution of obtained cDNA were assessed by gel electrophoresis.

Array hybridization and data analysis

mRNA isolated and amplified in three independent experiments was hybridized to GeneChip *C. elegans* Genome Arrays containing 22,500 predicted transcripts. 5 µg of fragmented cDNA were used for each hybridization. The GeneSpring software was used to carry out data analysis. For the probe intensity values generated by the Affymetrix scanner, Robust Multichip Average algorithm was used for normalization and statistical processing. Data were then filtered to remove genes with low expression values (<10). t-test was performed to sequentially filter out genes with unreliable signal level between replicates ($p < 0.05$). Finally, genes were filtered for fold change.

RNAi

RNAi was performed as described using published clones (*14*). To screen the candidate genes, 4 L4 larvae were placed on seeded RNAi plates and their progeny screened after 4 days by dye filling.

Plasmid Constructions

Initial attempts to clone PCR-amplified *fig-1* cDNA into standard vectors failed to yield *E. coli* transformants with the expected inserts, apparently because the cDNA is toxic to *E. coli*. The toxicity problem was resolved by creating expression vector pMT1, which has minimal transcriptional activity. Specifically, the *Sph*I-*Apa*I fragment of pPD95-75 (*15*) was replaced with pBS-KS Multiple Cloning Site Region without flanking T7 and T3 promoters. To facilitate cDNA expression, the *unc-54* 3'UTR was amplified by PCR from pPD95-75 and the resulting amplicon was ligated to the above plasmid digested with *Sal*I and *Apa*I.

FIG-1 isoforms: Two predicted isoforms of F53B7.5 (*fig-1*) are annotated (wormbase.org, release 190). While we could isolate cDNA for the short isoform, we could not amplify cDNA of the long isoform. PCR-amplification from several cDNA libraries resulted in isolation of clones that contained the last 4 exons spliced to each other, but these were not properly spliced to the rest of the gene and should not result in

successful translation. Conservation of these last 4 exons in other species leads us to believe that they are likely to be part of the gene locus. It is possible that the long form is only spliced under certain conditions which were not represented in the animals used to make the cDNA libraries.

For pMT2, *fig-1* cDNA (short) was amplified by PCR from cDNA and digested with *Not*I and *Xho*I. The resulting amplicon was ligated to pMT1 digested with *Not*I and *Sal*I.

For $P_{fig\text{-}1}$GFP (pMT3), we PCR-amplified a 5.2 kb genomic DNA fragment containing sequences upstream of the *fig-1* ATG. The resulting amplicon was ligated to pPD95-75 digested with *Sph*I and *Kpn*I. This construct also gave faint expression in two pairs of ventral cord projecting neurons. This neuronal expression is not seen when using a 2.2 kb promoter region.

For $P_{F16F9.3}$GFP (pMT4), we PCR-amplified a 2 kb genomic DNA fragment containing sequences upstream of the predicted ATG. The resulting amplicon was ligated to pPD95-75 digested with *Hind*III and *Kpn*I.

For $P_{F53F4.13}$GFP (pMT5), we PCR-amplified a 650 bp genomic DNA fragment containing sequences upstream of the predicted ATG. The resulting amplicon was ligated to pPD95-75 digested with *Hind*III and *Kpn*I.

For $P_{T02B11.3}$GFP (pMT6), we PCR-amplified a 2.5 kb genomic DNA fragment containing sequences upstream of the predicted ATG. The resulting amplicon was ligated to pPD95-75 digested with *Sph*I and *Kpn*I.

For $P_{F11C7.2}$GFP (pMT7), we PCR-amplified a 350 bp genomic DNA fragment containing sequences upstream of the predicted ATG. The resulting amplicon was ligated to pPD95-75 digested with *Hind*III and *Kpn*I.

For $P_{fig\text{-}1}$*fig-1* (pMT8), we PCR-amplified a 2.2kb genomic DNA fragment containing sequences upstream of *fig-1* ATG. The resulting amplicon was ligated to pMT2 digested with *Sac*I and *Not*I.

For $P_{sra\text{-}6}$*fig-1* (pMT10), we PCR-amplified a 2.4kb genomic DNA fragment containing sequences upstream of *sra-6* ATG. The resulting amplicon was ligated to pMT2 digested with *Sac*I and *Not*I.

For $P_{T02B11.3}$*fig-1* (pMT11), we PCR-amplified a 2.5kb genomic DNA fragment containing sequences upstream of the predicted ATG. The resulting amplicon was ligated to pMT2 digested with *Sac*I and *Not*I.

For $P_{fig\text{-}1}$*fig-1* long (pMT15), we PCR-amplified the genomic region containing the last 5 exons of *fig-1* (long isoform). This was ligated into pMT8 taking advantage of an endogenous *BspE*I site in the last exon of the short isoform.

For $P_{F16F9.3}$DT-A(G53E) (pTB29), we performed site-directed mutagenesis on pJF142 [$P_{unc\text{-}122}$DT-A(K52E)], a gift of Hanna Fares (*16*), to obtain the diphtheria toxin A G53E mutant. Additionally, we found that DT-A also contained the D79G mutation. The 2056 bp region upstream of the F16F9.3 start site (-2057 to -1, relative to the ATG), was PCR-amplified and ligated as a *Pst*I/*BamH*I fragment into the vector generated by site-directed mutagenesis.

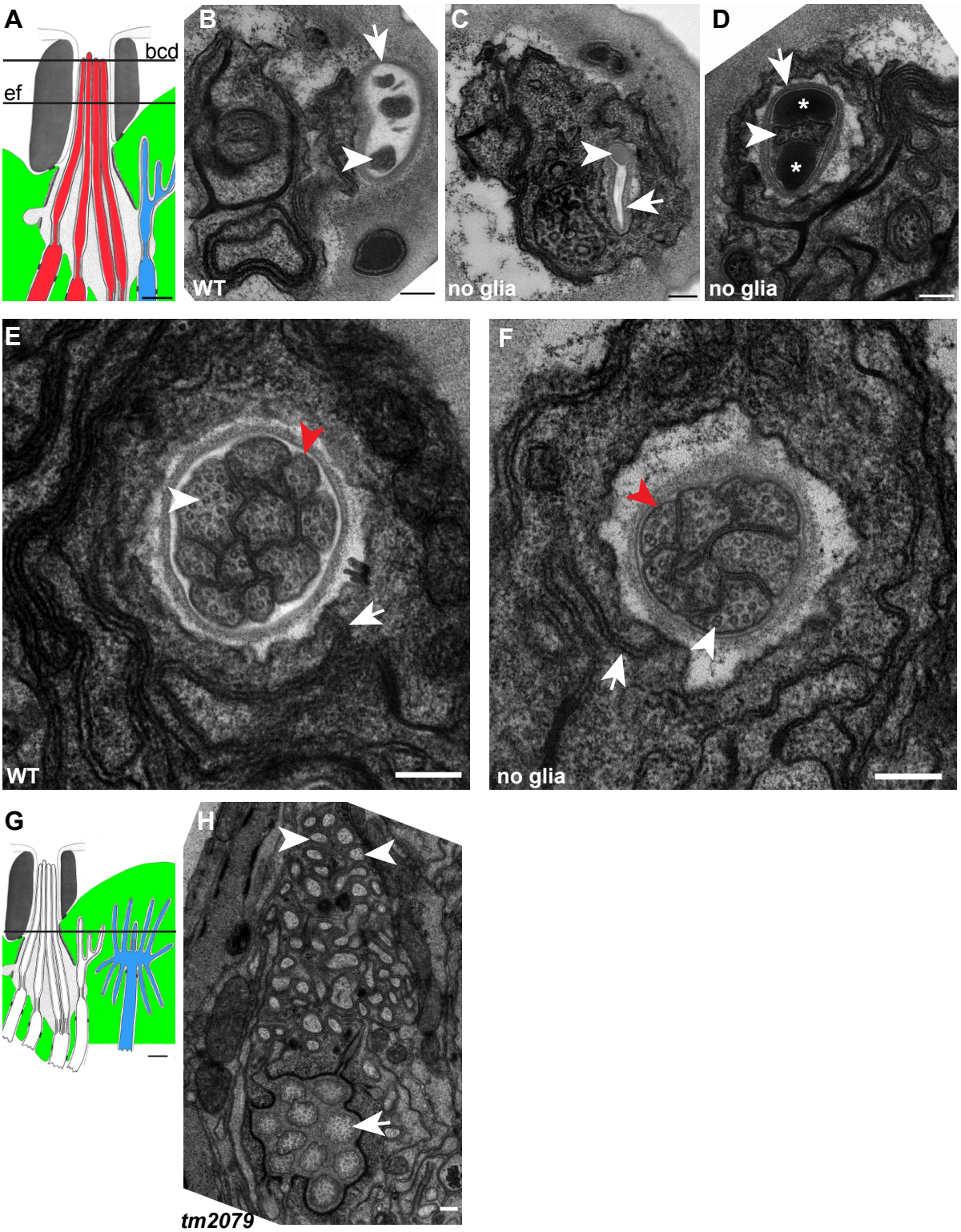

Fig. S1. Channel neuron cilia are not affected by glia removal. (**A**) A schematic depiction of the amphid opening indicating the level of the cross sections in **B** to **F**. Adapted from *(18)*.

Sheath glia, green; socket glia forming the pore, dark grey; channel neurons, red; sheath embedded neurons, blue. In the cartoons, anterior is up, scale bar, 1 μm. (**B**) The amphid opening of a wild-type animal. The beginning of a cilium (arrowhead) is seen in the cuticle-bound channel (arrow). (**C**) A glia-ablated animal in which the amphid channel appears open. (**D**) Another glia-ablated animal in which the beginning of a cilium is seen (arrowhead). An abnormal EM-dense matrix (asterisk) is seen within the channel. This matrix does not cause the dye-filling defects observed in glia-ablated animals as in some animals the socket channel is unobstructed (see **C**) but 100% of the animals are dye-filling defective. Furthermore, the channel opening is completely normal in *fig-1(tm2079)* mutants, which also exhibit dye filling defects. This matrix is also not the cause of the behavioral defects observed, as glia-ablated animals are defective in avoidance of volatile compounds such as 1-octanol which do not require an open channel for entry. Specifically, we tested *daf-6(e1377)* animals, in which the channel cilia cannot access the environment and are embedded within the sheath (*17*), and found them to avoid 1-octanol (chemotaxis index -0.43) much better than glia-ablated animals (average chemotaxis index -0.10). (**E**) Wild-type channel cilia (red arrowhead) displaying the proper microtubule (arrowhead) arrangement. Note that the amphid socket glia is not affected by the ablation. The characteristic junction that the socket forms unto itself is indicated by the arrow. (**F**) Glia-ablated animals also have normal channel cilia (red arrowhead) with normal microtubules (arrowhead). (**G**) Amphid cartoon with the AFD neuron shown in blue, note the villi-like projections at the level of the cross section. (**H**) In *fig-1(tm2079)* animals, the AFD villi appear normal (arrowhead) as do the channel cilia (arrow). In EM images, dorsal is up; scale bar, 200 nm.

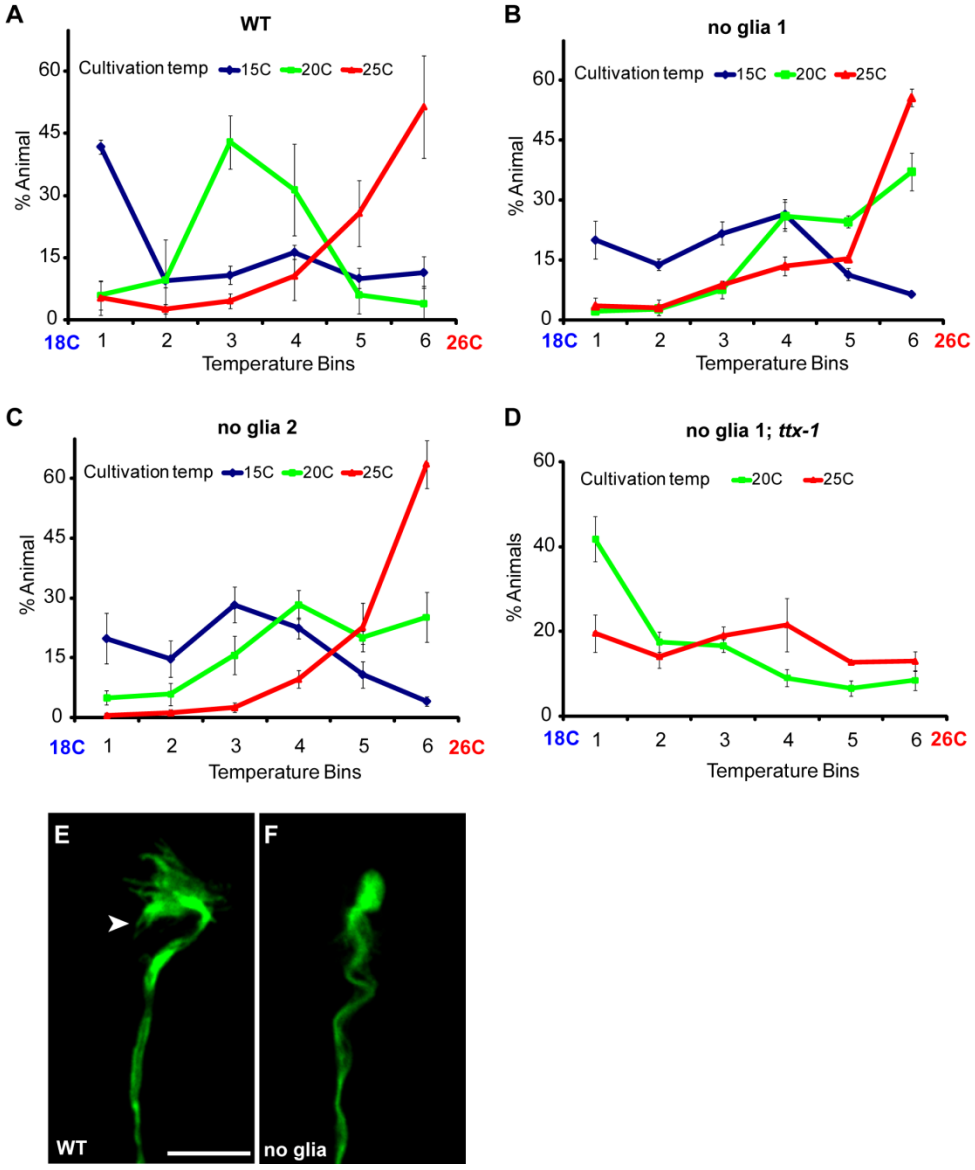

Fig. S2. AFD functional and morphological defects in glia ablated animals. (**A**) Thermotaxis profile of wild-type animals cultivated at three different temperatures. (**B** and **C**) Glia ablated animals fail to migrate to their cultivation temperature, especially if grown at 20°C, and thermotax to warmer temperatures. (**D**) Glia-ablated *ttx-1(p767)* animals migrate to cold temperatures, the reported behavior of *ttx-1(p767)* animals. (**E** and **F**) Glia-ablated animals lack the AFD villi seen in wild-type animals (arrowhead). Scale bar, 5 μm.

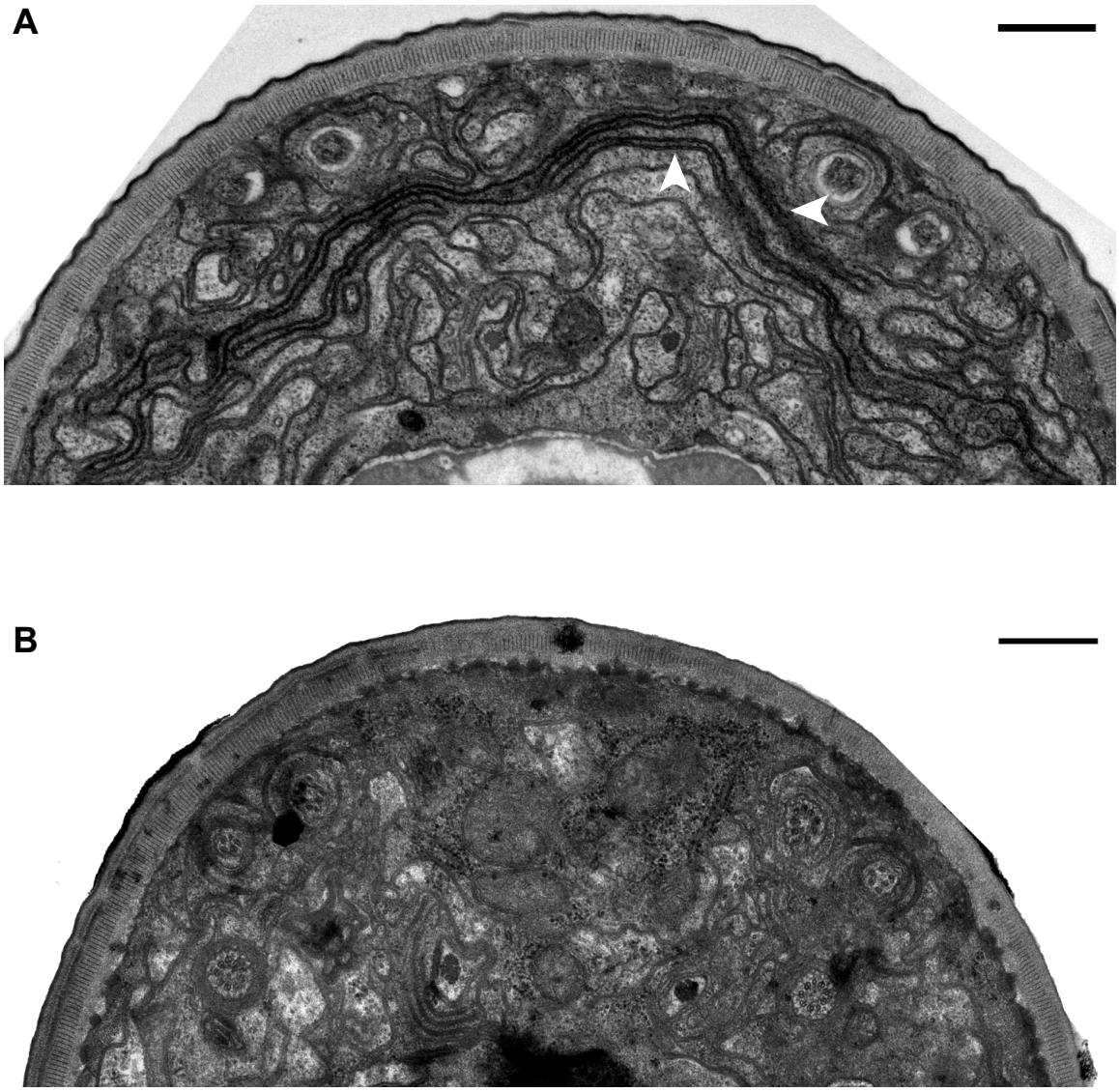

Fig. S3. AWC fails to extend wing-like cilia during dauer in absence of glia. (**A**) EM image of a wild-type dauer animal in cross section. Two overlapping AWC wings can be seen, arrowheads. (**B**) A glia-ablated animal (*nsIs109*) at the same cross section level has no AWC cilia extensions. Dorsal is up. Scale bar, 500 nm.

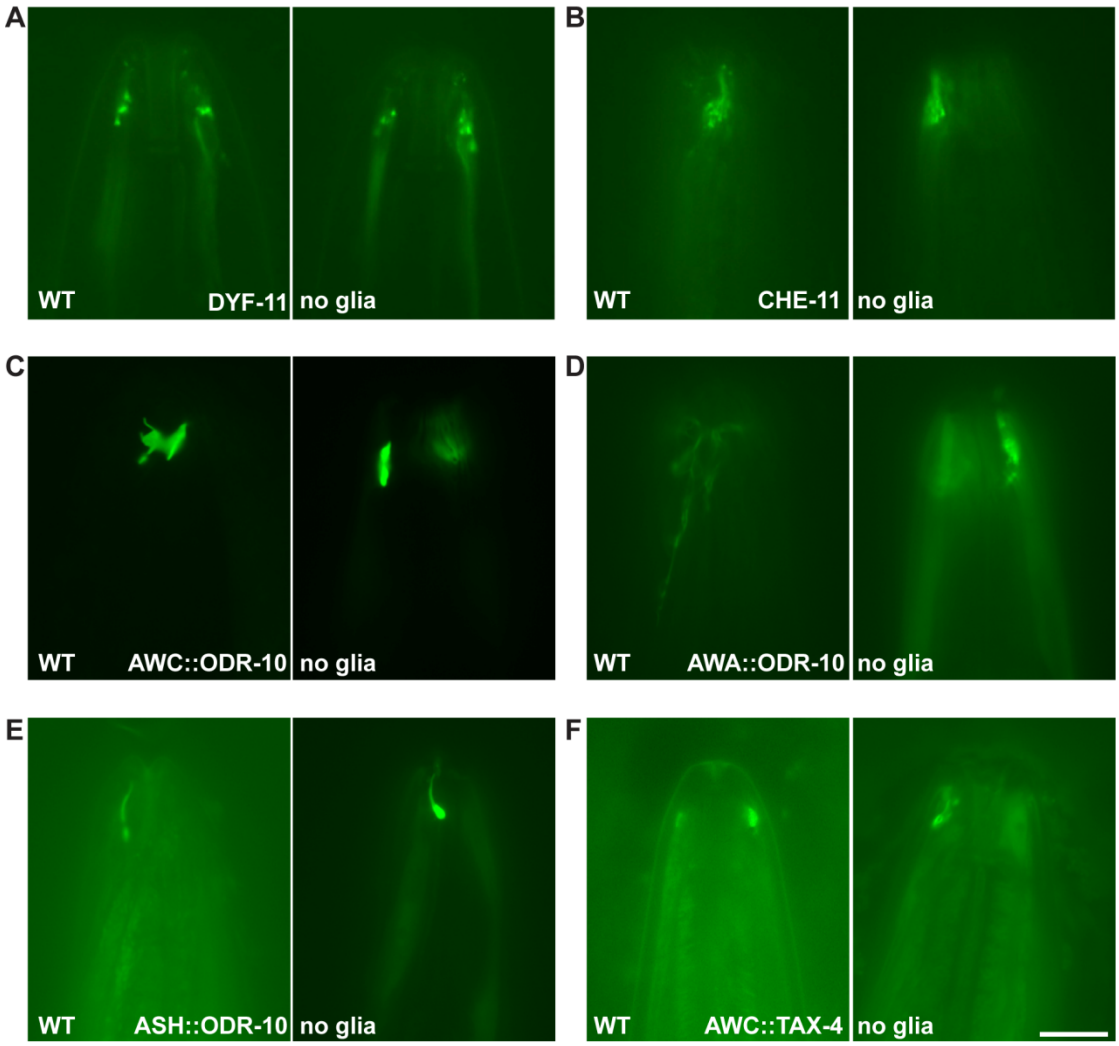

Fig. S4. Cilia components localize properly in absence of glia. (**A**) DYF-11, an IFT-B particle component (*19*) and (**B**) CHE-11, an IFT-A particle component (*20*), localize normally in amphid cilia of glia-ablated animals. ODR-10, an odorant receptor (*21*), localizes normally when expressed in the AWC (**C**), AWA (**D**), or ASH (**E**) cilia of glia-ablated animals. (**F**) TAX-4, a cyclic nucleotide gated channel subunit (*22*), localizes normally in glia-ablated animals. Anterior is up, scale bar 10 μm.

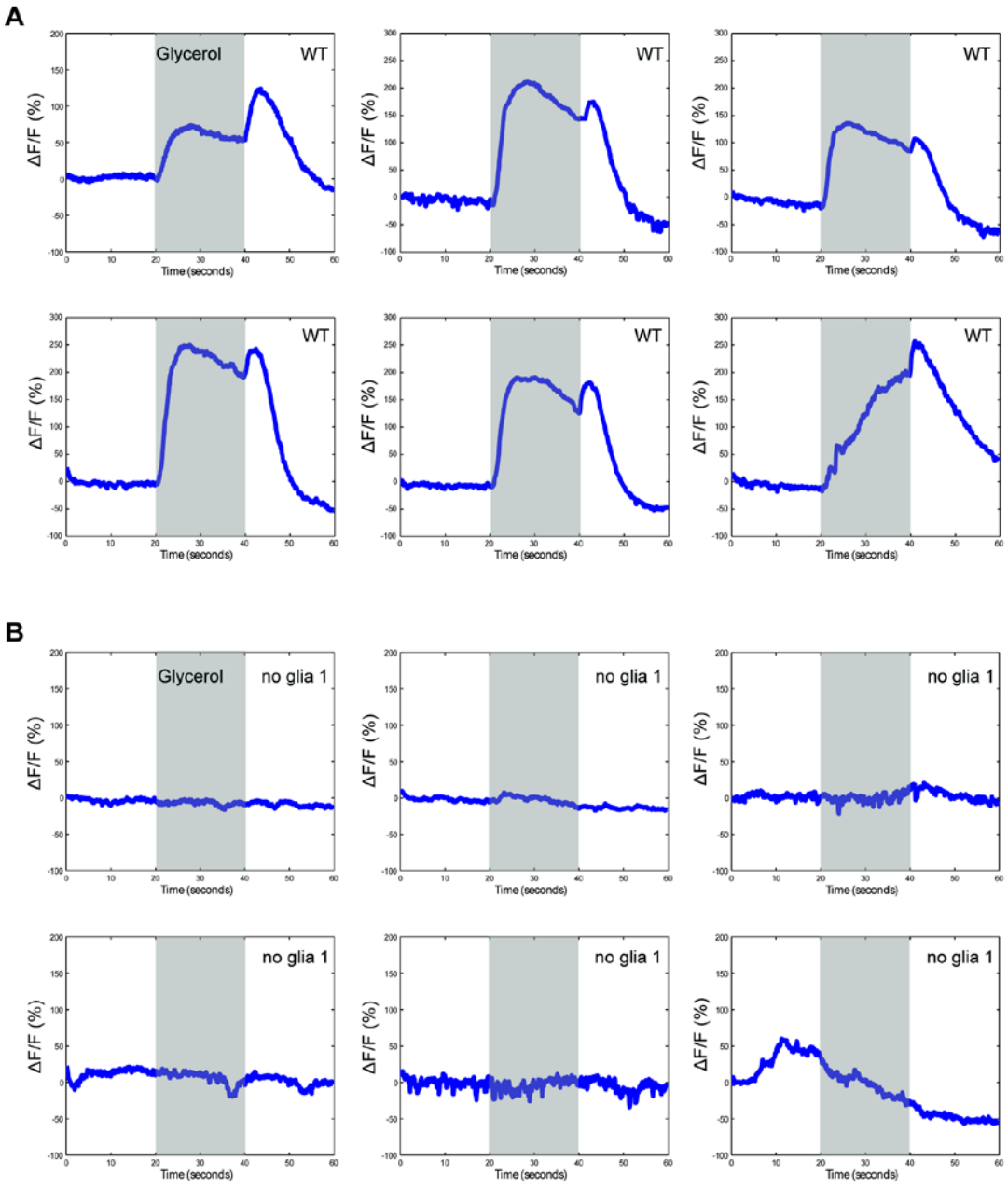

Fig. S5. Glia are required for Ca^{2+} changes in ASH. (**A**) Six traces of G-CaMP fluorescence in the ASH neuron of different animals exposed to 1M glycerol. Stimulus is presented during the shaded region. (**B**) In absence of glia, no G-CaMP changes are observed as a result of stimulus application.

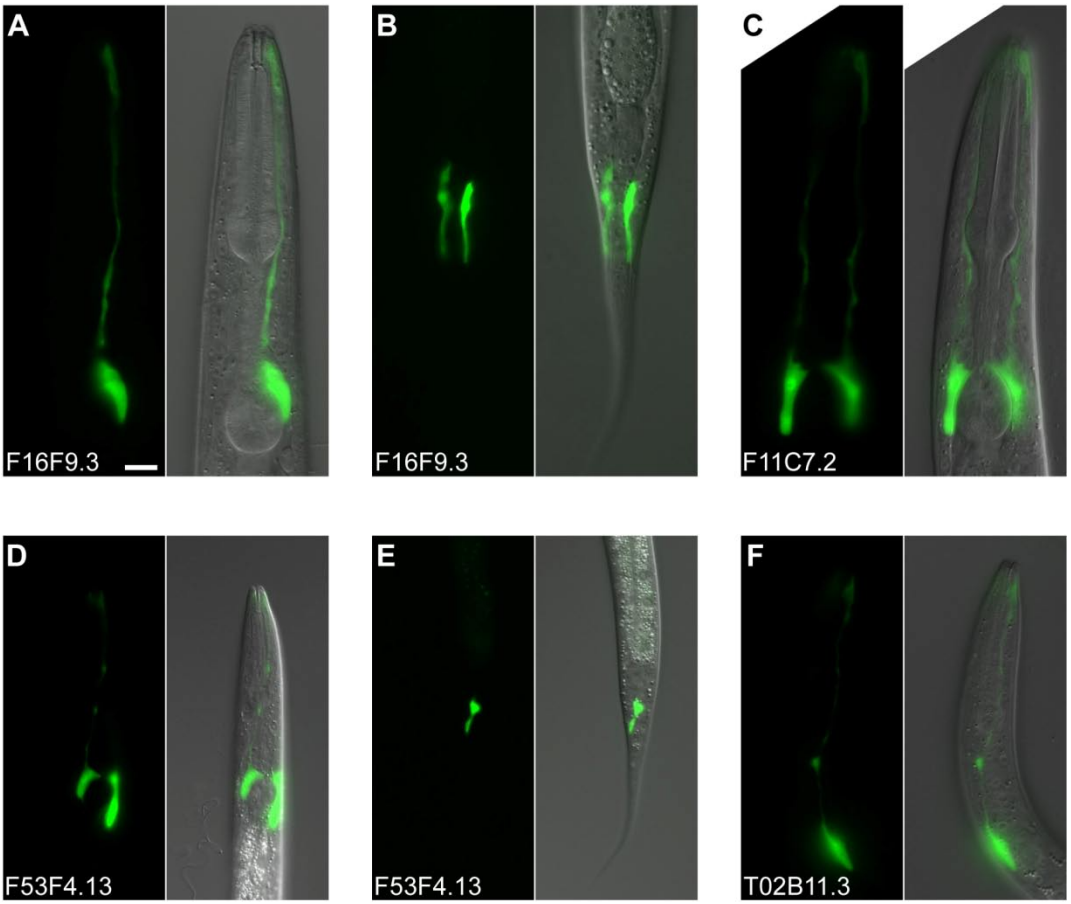

Fig. S6. Expression pattern of sheath-enriched genes. (**A** and **B**) F16F9.3, the most enriched gene in the microarray, is expressed only in amphid (**A**) and phasmid (**B**) sheath glia. (**C** to **F**) F11C7.2, F53F4.13 and T02B11.3 promoter fusion constructs are also expressed in amphid and phasmid sheath glia. Anterior is up, scale bar, 10 μm.

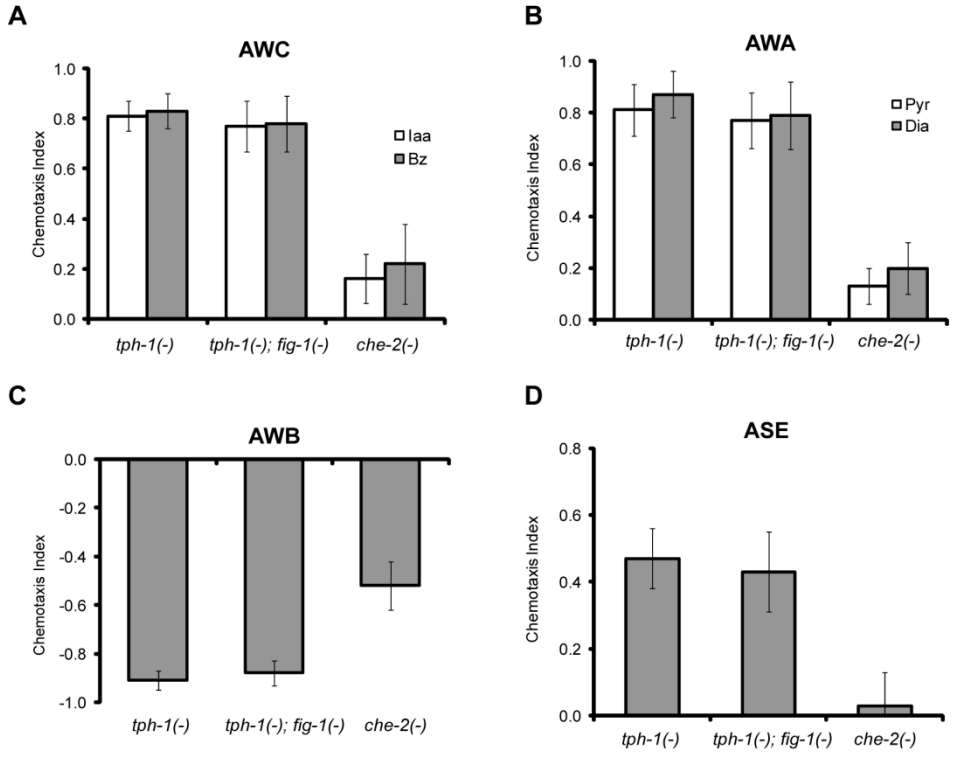

Fig. S7. *fig-1* mutants are normal for some odortaxis and chemotaxis behaviors. AWC (**A**), AWA (**B**), AWB (**C**), and ASE (**D**) function is not affected in *fig-1(tm2079)* animals. *fig-1(tm2079)* animals are sluggish. We found that this defect could be suppressed by *tph-1(mg280)*, a gene required for serotonin synthesis. As chemotaxis results are difficult to interpret if the animals have locomotory defects, we performed these assays in the *tph-1(mg280)* background. *che-2*, *che-2(e1033)* chemosensory mutants; error bars, standard deviation of 8 or more assays

Table S1. Amphid sheath glia enriched mRNAs. Genes enriched more than 4-fold are shown. The transgene used to label sheath glia, *vap-1::GFP*, expresses faintly in AFD also. The Affymetrix microarray probe used is included (Affy probe). TM, predicted transmembrane or secreted protein.

Gene name	Locus	Affy Probe	Fold	Description	TM
F16F9.3		181258_at	416	small secreted peptide with a Calcium-binding EF-hand domain	Y
F14D7.7		178799_at	329	similarit to Chlorobium tepidum Peptidyl-prolyl cis-trans isomerase	Y
T02B11.4		186124_at	307	Small secreted protein with conserved cysteines	Y
T02B11.3		174051_s_at	222	Small secreted protein with conserved cysteines	Y
"		185805_at	38.0		
F53F4.13		182491_at	177	integral membrane protein	Y
F53B7.5		173307_s_at	163	thrombospondin, type I and C6 repeat containg protein, secreted protein	Y
"		191533_s_at	27.6		
R05A10.3		183692_s_at	134	contains similarity to S. cerevisiae Conserved Oligomeric Golgi complex 1	Y
R05A10.4		183248_at	132	contains similarity to Pfam domain PF07403 Protein of unknown function (DUF1505) contains similarity to Interpro domain IPR009981 (Protein of unknown function DUF1505)	Y
R13D7.2		176714_at	101	contains similarity to Pfam domain PF03236 Domain of unknown function DUF263 contains similarity to Interpro domain IPR004920 (Protein of unknown function DUF263)	
F15D4.7		179655_at	96.7	transposon	
F52E1.2		180478_at	91.1	contains similarity to Pfam domain PF00059 Lectin C-type domain	Y
C33G8.4		183569_at	83.8	putative secreted or extracellular protein family member precursor	Y
F07C6.3		177784_at	83.6	transmembrane protein	Y
R07A4.4		178781_at	68.7	contains similarity to Thrombospondin, type I, IPR003609 (Apple-like), IPR003014 (N/apple PAN), IPR008266 (Tyrosine protein kinase, active site)	Y
C08F11.1		184129_at	68.2	putative secreted or extracellular protein family member precursor	Y
R06F6.11	tag-209	187447_at	64.7	putative secreted or extracellular protein precursor	Y
Y54G2A.10		174184_at	63.2	putative secreted or extracellular protein precursor	Y
ZK822.4		178629_at	61.8	contains similarity to Pfam domain PF02520 Domain of unknown function DUF148 contains similarity to Interpro domain IPR003677 (Protein of unknown function DUF148)	
F11C7.3	vap-1	182409_s_at	61.7	vap-1 encodes a predicted secreted protein that is similar to the venom allergen-like proteins found in a number of invertebrates, including parasitic nematodes	Y

Gene name	Locus	Affy Probe	Fold	Description	TM
"		171730_x_at	55.8		
"		172026_x_at	37.7		
C44H4.1		193311_at	58.6	Leucine Rich Repeat (2 copies) (6 domains)	Y
R05A10.2		182944_at	56.6	contains similarity to Saccharomyces cerevisiae Actin-binding protein that stabilizes actin filaments; Tpm1,	Y
F35B12.9		193419_at	55.7	contains similarity to Homo sapiens Titin; TR:Q8WZ42	Y
Y69H2.3		177839_s_at	53.4	trypsin inhibitor-like, cysteine-rich TIL region precursor family member, Fibrillins and related proteins containing Ca2+-binding EGF-like domains	Y
Y23H5B.3		176889_at	52.8	putative secreted or extracellular protein precursor	Y
C05B5.9		189071_at	46.1	pseudogene	
Y46B2A.2		189905_s_at	44.3	DNA helicase PIF1/RRM3	
F11C7.2		182121_at	43.6	thrombospondin, type I family member. Secreted or transmembrane	Y
F20A1.1		172426_x_at	43.3	putative secreted or extracellular protein family member precursor	Y
F59A7.2		183014_at	38.7	putative secreted or extracellular protein family member precursor	Y
K09B3.1		181495_at	37.3	metalloproteinase 1 like, Metridin-like ShK toxin;ShK domain-like	Y
Y69A2AR.22		176280_at	37.2		Y
T02B11.7	nas-32	188595_s_at	36.6	metalloprotease III family member	Y
Y38H6A.3		182558_at	35.8	contains similarity to Interpro domain IPR006150 (Cysteine-rich repeat)	Y
K06A9.1		194259_x_at	34.8	homolog of human TCOF1, which when mutated leads to Treacher-Collins syndrome (OMIM:154500).	Y
"		184777_s_at	12.0		
"		172070_x_at	7.24		
F58B4.1a	nas-31	189892_at	34.7	Meprin A metalloprotease	Y
F14D2.7		180618_at	30.6	Zinc finger, Rad18-type putative	Y
K11E4.1		179237_at	29.8	integral membrane protein, contains similarity to Pfam domain PF01764 (Lipase (class 3)	Y
F35E2.5		177877_at	28.6	contains similarity to Pfam domain PF03761 Domain of unknown function (DUF316) contains similarity to Interpro domain IPR005514 (Protein of unknown function DUF316)	Y
F40F8.4		178505_s_at	27.5	putative secreted or extracellular protein precursor with WD40 repeat	Y
C25E10.11		187011_at	26.9	putative secreted or extracellular protein	Y
C37E2.5	ceh-37	192014_s_at	26.3	ceh-37 has an OTX-like homeodomain but lacks other domains found in OTX proteins, and the CEH-37 homeodomain is predicted to resemble the Myb domain of telomere-binding proteins; CEH-37 binds the telomeric sequence 'TTAGGC	
"		173897_at	5.18		
Y105C5B.5		185106_at	25.0		

Gene name	Locus	Affy Probe	Fold	Description	TM
F59A7.5		183007_at	24.5	putative secreted or transmembrane protein	Y
C56E10.3		185563_at	24.2	contains similarity to Drosophila melanogaster Flybase gene name is CLIP-190-PA, FLYBASE:CG50	
"		172586_at	11.0		
B0285.6		190632_at	23.6	predicted sodium-coupled carboxylate transporter related to Drosophila Indy and the mammalian NaDC1 and NaDC3 transporters	Y
C56C10.4		184220_at	23.5	contains similarity to Pfam domain PF01682 DB module contains similarity to Interpro domain IPR002602	Y
C12D8.9		179347_at	23.4		
C05D12.1		184125_at	22.3	contains similarity to Interpro domains IPR005018 (DOMON related), IPR003006 (Immunoglobulin/major histocompatibility complex, conserved site), IPR006593 (Cytochrome b561 / ferric reductase transmembrane)	Y
F13B6.3		180766_at	21.4	contains similarity to Homo sapiens Mucin-5AC precursor (Fragment)	Y
C23H3.7	tre-5	187729_s_at	20.8	trehalase (tre-5)	Y
F07F6.7		190471_at	20.5	apolipoprotein L like	Y
K02E11.3		181315_at	20.3	contains similarity to Interpro domain IPR002213 (UDP-glucuronosyl/UDP-glucosyltransferase)	Y
H22K11.1	asp-3	191956_at	20.0	asp-3 encodes an aspartyl protease homolog that is required, in parallel with ASP-4 but downstream of CLP-1 and TRA-3, for degenerative (necrotic-like) cell death in neurons induced by mutations such as mec-4(d), deg-3(d), or gsa-1(gf).	Y
K02E11.5		180905_at	18.3	UDP-glucuronosyl/UDP-glucosyltransferase	
C41C4.1		187005_at	18.3	contains similarity to Pfam domain PF04590 Protein of unknown function, DUF595 contains similarity to Interpro domain IPR007669 (Protein of unknown function DUF595)	Y
C06E2.2		182220_at	16.9		
F16H6.10		176708_at	16.8		
Y71G12B.17		176293_at	16.5	Phosphatidylinositol transfer protein [KOG3668]	
Y39H10A.1		176555_at	14.9	integral membrane protein	Y
T05C1.1		182235_at	14.7	putative protein, with a transmembrane domain, a coiled coil-4 domain (2E769), mRNA.	Y
K02E11.4		181328_at	14.6	contains similarity to Interpro domain IPR007110 (Immunoglobulin-like)	Y
Y73B6A.3		185418_at	14.6	putative secreted or extracellular protein family member precursor, UDP-glucuronosyl/UDP-glucosyltransferase;Histone H5	Y
F36H2.3		192520_s_at	14.5	Complement factor H precursor like	Y
T23C6.3		183310_s_at	13.5		
M01G12.14		185163_s_at	13.4	contains similarity to Rhizobium meliloti Putative transposase of insertion sequence ISRM19 protein	
E02H9.3		181022_s_at	13.0	contains similarity to Pfam domain PF03312 Protein of unknown function, DUF272 contains similarity to Interpro domain IPR004987	

Gene name	Locus	Affy Probe	Fold	Description	TM
C40H5.2		178802_at	12.4	contains similarity to Bifidobacterium longum Possible magnesium and cobalt transport protein.; TR:Q8G4E0	
F49F1.7		181132_s_at	12.3	contains similarity to Pfam domain PF01549 ShK domain-like contains similarity to Interpro domain IPR003582 (Metridin-like ShK toxin)	Y
H11L12.1		172299_x_at	12.1		
"		172550_x_at	10.1		
C16H3.2	lec-9	192336_at	12.0	lec-9 encodes a predicted lectin that affects embryonic viability.	
F59E11.2		185750_at	12.0	Short-chain dehydrogenase/reductase SDR;Glucose/ribitol dehydrogenase;Insect alcohol dehydrogenase family;NAD(P)-binding;short chain dehydrogenase	
C12C8.1	hsp-70	192266_s_at	11.8	hsp-70 encodes a heat-shock protein that is a member of the hsp70 family of molecular chaperones.	
F31F6.5	daf-6	187906_at	11.6	a Patched-like gene required for amphid sheath channel formation, daf-6 interacts genetically with che-14	Y
C27C7.1		172213_x_at	11.5	contains similarity to Homo sapiens Hypothetical protein FLJ13213	
C17E7.6	nhr-158	190925_at	11.5	nuclear receptor NHR-51 like family member	
F08G5.6		178843_at	11.3	CUB-like region; CUB-like domain	Y
T19H12.3		185822_s_at	11.3	putative secreted or extracellular protein family member precursor UDP-glucuronosyl/UDP-glucosyltransferase	Y
M03E7.2		181683_at	11.1	contains similarity to Plasmodium berghei 58 kDa phosphoprotein (Heat shock-related protein) (HRP).; SW:Q08168	Y
Y54F10BM.3		173344_at	10.8	Protein-tyrosine phosphatase, receptor/non-receptor type;Protein-tyrosine phosphatase;Protein-tyrosine phosphatase, catalytic	Y
C38D9.2		179425_at	10.6	Zinc finger, CCHC-type	
F59D6.7		180406_at	10.4	contains similarity to Pfam domain PF00036 EF hand contains similarity to Interpro domains IPR011992 (EF-Hand type), IPR002048 (Calcium-binding EF-hand), IPR008080 (Parvalbumin), IPR003299 (Flagellar calcium-binding protein (calflagin))	
F59D12.3		180289_at	10.4	contains similarity to Pfam domain PF04590 Protein of unknown function, DUF595 contains similarity to Interpro domain IPR007669 (Protein of unknown function DUF595)	Y
T13B5.9		175491_at	10.3	Peptidase M, neutral zinc metallopeptidases, zinc-binding site	
C25F9.2		178896_at	9.9	DNA polymerase type B, organellar and viral family member (5T899), predicted mRNA.	

Gene name	Locus	Affy Probe	Fold	Description	TM
F10A3.1		177627_at	9.8	claudin homolog that may be required for normal cohesion of apical junctions in epithelia; F10A3.1 is worm-specific, with obvious homologs only in C. elegans	Y
K02A2.3	kcc-3	193537_s_at	9.7	Bumetanide-sensitive Na-K-C1 cotransporter	Y
C25A1.2	fkh-10	190179_at	9.7	fkh-10 encodes one of 15 forkhead transcription factors	
W01A11.4	lec-10	190281_at	9.6	lec-10 encodes a galectin, a soluble galactose-binding lectin; recombinant lec-10 can bind to sugar in an in vitro assay.	
W06D11.3		183074_at	9.6	Homologous to E. coli RecQ and human BLM and WRN proteins that are defective in Bloom's syndrome and Werner's syndrome	
C11H1.9		177796_at	9.4	contains similarity to Pfam domain PF01105 emp24/gp25L/p24 family/GOLD contains similarity to Interpro domains IPR001251 (Cellular retinaldehyde-binding/triple function, C-terminal), IPR000348 (emp24/gp25L/p24)	Y
C14F11.5	hsp-43	190097_s_at	9.4	heat shock protein	
Y38H6C.7		181511_at	9.3	pseudogene	
F21H12.4	ptc-2	193368_s_at	9.3	PATCHED homolog, has sterol sensing domain (SSD); PTC-2 is required for normal fat storage, normal egg osmotic integrity, locomotion, egg laying, and viability in RNAi assays	Y
K12H4.1	ceh-26	176620_at	9.3	ceh-26 encodes a protein that contains a prospero-related homeodomain; expressed in nuclei of the adult head, tail neurons, and one cell in the postdeirids.	
K10C2.3		189595_s_at	9.3	aspartic proteinase family member	Y
C14F11.6		193712_s_at	9.1	DTDP-4-dehydrorhamnose 3,5-epimerase (RFBC gene)	
T04A11.1		182091_s_at	9.1	Phenazine biosynthesis PhzC/PhzF protein;Phenazine biosynthesis-like protein	
Y55B1BL.1		186903_at	9.1	integral membrane protein	Y
F53F4.6	rdy-2	178699_at	9.1	RDY-2 (rod-like lethal Dye-filling defective); contains similarity to Interpro domain IPR017441 (Protein kinase ATP binding, conserved site)	Y
C05B5.3	pqn-8	186853_s_at	8.9	glutamine/asparagine (Q/N)-rich ('prion') domain	Y
C38D9.5		178878_at	8.9	BRCT;Ankyrin;Protein of unknown function WSN;Domain of unknown function	Y
C56C10.6		189105_s_at	8.8	Casein kinase	
C33C12.3		189972_at	8.5	contains similarity to Pfam domain PF02055 O-Glycosyl hydrolase family 30 contains similarity to Interpro domains IPR017853 (Glycoside hydrolase, catalytic core)	Y
Y46C8AL.2	clec-174	172185_x_at	8.4	C-type lectin	Y
R05D7.5		178659_at	8.3	putative membrane protein	Y
Y57E12B.3		176402_at	8.2	contains similarity to Pfam domains PF04083 (ab-hydrolase associated lipase region), IPR000073 (Alpha/beta hydrolase fold-1), IPR000694 (Proline-rich region)	Y

Gene name	Locus	Affy Probe	Fold	Description	TM
Y6E2A.4		179418_at	8.1	contains similarity to Pfam domains PF00104 (Ligand-binding domain of nuclear hormone receptor) , PF00105 (Zinc finger, C4 type (two domains))	
Y65B4BL.2	deps-1	186952_at	8.0	unfamiliar P-granule-associated protein required for germline RNAi, orthologs in other Caenorhabditis species, but has no non-nematode orthologs.	
Y110A2AL.4		187531_at	8.0	putative membrane protein	Y
"		175367_s_at	6.7		
F32B5.4		183820_at	8.0	putative membrane protein	Y
F29B9.9	col-111	188461_s_at	7.9	COLlagen structural gene	Y
Y69H2.1		177981_at	7.9	contains similarity to Myxine glutinosa NADH-ubiquinone oxidoreductase chain 4	Y
C05B5.8		186950_at	7.8	contains similarity to Shigella flexneri Putative transport protein.; TR:Q83RB7	Y
F14D2.4	bath-29	181360_s_at	7.8	Meprin/TRAF-like MATH and BTB/POZ domain containing protein family member	
"		181302_s_at	6.1		
T13C2.2		179776_at	7.6		Y
"		180200_at	5.6		
C17C3.5		183228_at	7.6	Protein of unknown function DUF38, Caenorhabditis species;FTH domain	
R09H3.3		179945_at	7.5		
W09B6.5		181510_at	7.4		
ZC449.2		183234_s_at	7.4	PAN domain and Apple-like domain, secreted or transmembrane	Y
"		191797_at	6.1		
C12D5.7	cyp-33A1	189430_at	7.4	cytochrome p450 2C33v4 family member (5I160)	Y
C17E7.9		175231_s_at	7.3	integral membrane protein	Y
C04F12.9	rnh-1.3	184160_at	7.3	ribonuclease H	
Y105C5A.25		187110_at	7.3	pseudogene	
F59H6.5		185671_s_at	7.3	contains similarity to Pfam domain PF05970 Eukaryotic protein of unknown function (DUF889) contains similarity to Interpro domains IPR010285 (Protein of unknown function DUF889, eukaryote), IPR003593 (AAA+ ATPase, core), IPR006034 (Asparaginase/glutaminase)	
C34D4.10		181223_at	7.2		Y
C49A9.4		182898_at	7.1	orthologous to the human gene CYSTATIN B (STEFIN B) (CSTB; OMIM:601145), which when mutated leads to disease.	
C10H11.10	kca-1	186482_s_at	7.1		
T04G9.7		179805_s_at	7.1		Y
"		174857_at	6.0		
C28H8.11		192112_s_at	7.0	Tryptophan 2,3-dioxygenase	
Y38H6C.8		193307_at	7.0	Lectin C-type domain short and long forms	Y
T14G8.4		179625_at	7.0	contains similarity to Mus musculus Gamma-tubulin complex component GCP5 homolog.; TR:Q8BKN5	Y
F59B1.2		182919_at	7.0		Y

Gene name	Locus	Affy Probe	Fold	Description	TM
F58B6.2	inft-1	183953_at	7.0	Proline-rich region;Actin-binding FH2 and DRF autoregulatory;Actin-binding FH2;Formin Homology 2 Domain	
Y65B4BR.8		175375_at	6.8	contains similarity to Pfam domain PF06425 Partner of SLD five, PSF3 contains similarity to Interpro domain IPR010492 (GINS complex, Psf3 component)	
Y38E10A.12		172624_x_at	6.8	contains similarity to Pfam domain PF07203 Protein of unknown function (DUF1412) contains similarity to Interpro domain IPR009853 (Protein of unknown function DUF1412)	Y
Y43F8C.1	nlp-25	183895_at	6.8	Neuropeptide-Like Protein (prion protein)	Y
F40G12.5		180606_at	6.7	Protein of unknown function DUF263;Domain of unknown function DUF263	Y
T05F1.7		178341_at	6.7	contains similarity to Paramecium tetraurelia Chromosome undetermined scaffold_33, whole genome shotgun sequence.; TR:A0D056	
F20A1.10		186043_at	6.7	putative secreted protein	Y
F53A9.8		180612_s_at	6.7	contains similarity to Plasmodium chabaudi Pc-fam-3 protein putative (Fragment).; TR:Q4XGP3	
Y39E4B.12	gly-5	187815_s_at	6.7	gly-5 encodes a predicted member of the UDP-GalNAc:polypeptide N-acetylgalactosaminyltransferase (ppGaNTase) family.	Y
T27F2.4		179204_s_at	6.7	Basic-leucine zipper (bZIP) transcription factor	
Y57G7A.5		184542_at	6.7		
F20A1.9		183123_s_at	6.6	B302, (SPRY)-like;SPla/RYanodine receptor SPRY;ATPase associated with various cellular activities, AAA-4;SPRY domain;Divergent AAA domain	
T16G1.5		179610_s_at	6.5	Protein of unknown function DUF227;Protein kinase-like;Protein of unknown function DUF1679, Caenorhabditis species;CHK kinase-like;Protein of unknown function (DUF1679);Domain of unknown function (DUF227)	
T06C12.4	fbxa-197	182533_at	6.5	Protein of unknown function DUF38, Caenorhabditis species;FTH domain	
C17H12.12		186931_at	6.5	BTB/POZ-like	
ZK265.2	col-63	173650_s_at	6.5	COLlagen structural gene (37.4 kD) (col-63)	Y
T05E11.8		179794_at	6.5	contains similarity to Pfam domain PF02520 Domain of unknown function DUF148 contains similarity to Interpro domain IPR003677 (Protein of unknown function DUF148)	Y
C04B4.2		179273_at	6.3	Calcium-binding EF-hand	
H06H21.1	srw-94	184731_at	6.3	7TM chemoreceptor, srw family	Y
B0280.12b	glr-2	189724_at	6.3	glr-2 encodes an AMPA (non-NMDA)-type ionotropic glutamate receptor subunit	Y
Y37D8A.23	unc-25	194006_at	6.3	GABA neurotransmitter biosynthetic enzyme, glutamic acid decarboxylase (GAD); unc-25 activity is required for GABA synthesis	
Y43F8B.9		180823_at	6.3		

Gene name	Locus	Affy Probe	Fold	Description	TM
T21G5.3	glh-1	190711_at	6.2	a putative DEAD-box RNA helicase that contains four CCHC zinc fingers and is homologous to Drosophila VASA, a germ-line-specific, ATP-dependent RNA helicase	
F26A1.9		184151_at	6.2		
Y39A3B.3		184691_at	6.2	integral membrane protein	Y
C05D2.8		187761_s_at	6.2		Y
B0034.4		187363_at	6.1		Y
Y8G1A.2	inx-13	193448_s_at	6.0	inx-13 encodes an innexin, an integral transmembrane channel protein that is a structural component of invertebrate gap junctions	Y
F10C1.2	ifb-1	192149_s_at	6.0	ifb-1 (also known as vab-21) encodes two isoforms of an essential intermediate filament protein that is coexpressed with the essential IF proteins IFA-1, IFA-2, and IFA-3, along with IFA-4	
"		175020_at	5.2		
F14B4.1		174848_s_at	6.0	LDL receptor-related protein	Y
H02I12.1		180976_s_at	5.9	protein with 12 chitin-binding peritrophin-A domains; H02I12.1(RNAi) animals have an osmotically-sensitive embryonic lethal phenotype, perhaps because of defects in chitin and eggshell synthesis	Y
F53B2.3	eak-4	178868_at	5.9	eak-4 encodes a novel protein that contains an N-myristoylation signal; eak-4 acts in parallel to akt-1 to regulate insulin-like signaling and dauer formation	Y
C14F5.2	zig-3	192500_at	5.8	zig-3 encodes a predicted secreted protein that is a member of the immunoglobulin superfamily of proteins;	Y
Y97E10B.6	srx-11	187148_at	5.8	pseudogene	
F56C11.2	ptr-11	171745_x_at	5.7	ptr-11 encodes a nematode-specific member of the sterol sensing domain (SSD) proteins, distantly paralogous to Drosophila PATCHED (PTC) and human PTCH (OMIM:601309)	Y
M01G12.9		179942_at	5.7		
F33D4.2	itr-1	193676_s_at	5.7	inositol (1,4,5) trisphosphate receptor that affects the defecation cycle and pharyngeal pumping, and also affects ovulation in a pathway downstream of LET-23; interacts with UNC-54 in vivo	Y
H38K22.5	gly-6	175655_s_at	5.7	Glycosyl transferases	Y
R09H3.2		172250_x_at	5.7	probe is in intergenic region	
F31C3.10	rrn-3.56	173281_s_at	5.6	ribosomal RNA	
F47C12.8		186276_at	5.6	contains similarity to Pfam domain PF05912 C. elegans protein of unknown function (DUF870) contains similarity to Interpro domain IPR008588 (Protein of unknown function DUF870)	Y
"		171767_x_at	4.8		
F20B6.8	hpk-1	180322_at	5.6	a predicted dual-specificity protein kinase with distant homology to the vertebrate protein kinase DYRK1A and the Drosophila homolog mini-brain	

Gene name	Locus	Affy Probe	Fold	Description	TM
ZK1037.5	nhr-247	194098_at	5.6	Ligand-binding domain of nuclear hormone receptors, Zinc finger, C4 type (two domains)	
F57A8.1		188628_at	5.5	ETS domain	
Y92C3B.1	kbp-4	177029_at	5.5	Tropomyosin	
Y67A10A.9		185683_at	5.5	claudin homolog, protein with at least 3 transmembrane domains	Y
"		173027_s_at	4.3		
F59H5.3	bath-12	183672_at	5.5	pseduogene (Meprin/TRAF-like MATH and BTB/POZ domain containing protein family member)	
T08G5.3		179131_at	5.5	contains similarity to Homo sapiens hypothetical protein	Y
R166.5	mnk-1	190356_at	5.5	serine/threonine kinase	
F21H7.2		173177_s_at	5.4	contains similarity to Homo sapiens Neurofilament heavy polypeptide	
"		178141_s_at	4.0		
ZK669.5		189359_s_at	5.4	ras oncogene family	
C39B5.2		182485_at	5.4	Cyclin-like F-box;F-box domain	
Y38E10A.15		172635_x_at	5.4	Protein of unknown function DUF1412; Protein of unknown function (DUF1412)	Y
C05D10.4		176149_at	5.4	sterile alpha motif SAM	
"		187862_at	5.2		
F35E12.6		180342_at	5.3	CUB; CUB-like region; CUB-like domain	Y
Y46H3A.2	hsp-16.41	188444_at	5.3	hsp-16.41 encodes a 16-kD heat shock protein (HSP) that is a member of the hsp16/hsp20/alphaB-crystallin (HSP16) family of heat shock proteins	
ZK20.2	kin-6	175005_at	5.3	kin-6 encodes a predicted tyrosine protein kinase.	Y
ZK488.2	nhr-90	189961_at	5.3	nuclear Hormone Receptor	
Y59E1B.1		185607_at	5.3	putative nuclear protein (XC497)	
C14C10.7	ttr-43	191018_at	5.3	ttr-43 - (TransThyretin-Related family domain) contains similarity to Interpro domain IPR001534 (Transthyretin-like)	Y
F53G12.3		184226_at	5.3	partial homolog of dual oxidase ('Ce-Duox2'), with an N-terminal peroxidase domain, two central calmodulin-binding EF hands, and a C-terminal superoxide-generating NADPH-oxidase domain	Y
C01B10.3		185295_s_at	5.3	a paralog of IPP-5, and thus may functionally overlap with ipp-5 in vivo.	
W03A5.4		183687_at	5.2	contains similarity to Homo sapiens Uncharacterized protein DLGAP1	
F49C5.8		172759_x_at	5.2	transposon	
Y75B12B.3		185413_at	5.2	contains similarity to Saccharomyces cerevisiae Mlp proteins restrict telomere length by influencing the Rif1-Tel1 pathway of telomerase regulation; also involved in the translocation of macromolecules between the nucleoplasm and the NPC	
F17C8.5	twk-6	187930_at	5.2	twk-6 encodes one of 44 C. elegans TWK (two-P domain K+) potassium channel subunits that contain two pore-forming domains and four transmembrane domains	Y

Gene name	Locus	Affy Probe	Fold	Description	TM
R02C2.4	nhr-204	191007_at	5.2	nuclear hormone receptor	Y
W04G5.2	rab-11.2	189771_at	5.2	RAB family member (rab-11.2)	Y
K08E5.3	mua-3	189800_s_at	5.1	Caenorhabditis elegans essential gene mua-3, transmembrane cell adhesion receptor precursor; matrix receptor, muscle attachment protein, MUscle Attachment abnormal	Y
R07B1.10	lec-8	175710_s_at	5.1	galectin (20.4 kD) (lec-8)	
F40F9.3		193047_at	5.1	contains similarity to Interpro domain IPR001478 (PDZ/DHR/GLGF)	
T21E8.3	pgp-8	189037_at	5.1	pgp-8 encodes an ATP-binding protein that is a member of the P-glycoprotein subclass of the ATP-binding cassette (ABC) transporter superfamily; transmembrane	Y
ZK355.5		183073_at	5.0	EGF receptor, L domain;Receptor L domain	Y
F25H5.8		178186_at	5.0	Protein of unknown function UPF0057;Uncharacterized protein family UPF0057	Y
Y71H2AM.22	twk-45	176220_at	5.0	twk-45 - (TWiK family of potassium channels)	Y
K04H4.2		174044_at	5.0	secreted, with an N-terminal chitin-binding peritrophin-A domain followed by up to 15 cysteine-rich domains; the general organization of K04H4.2 protein resembles that of T10E10.4	Y
C36C9.3	fbxa-170	180118_at	5.0	a protein containing an F-box and an FTH/DUF38 motif, which may also mediate protein-protein interaction.	
R10H10.4		183646_at	5.0	contains similarity to Arabidopsis thaliana T15B16.1 protein.; TR:Q9ZSH8	Y
Y57G11C.31		187086_at	5.0	Protein of unknown function DUF271; Protein of unknown function (DUF271)	Y
T24B8.6	hlh-3	192523_at	4.9	hlh-3 encodes a basic helix-loop-helix transcription factor homologous to Drosophila Achaete-scute	
Y46H3A.1	srt-42	184414_at	4.9	7TM chemoreceptor, srt family	Y
W02D7.3		180864_at	4.9		Y
R03H10.6		186074_at	4.8	Nucleic acid binding, OB-fold, tRNA/helicase-type;Nucleic acid-binding, OB-fold;Nucleic acid-binding, OB-fold-like;OB-fold nucleic acid binding domain	
T10D4.10	sri-43	191471_at	4.8	7TM chemoreceptor, sri family	Y
ZK470.1		183484_at	4.8	contains similarity to Interpro domain IPR007248 (Mpv17/PMP22)	Y
K05B2.3	ifa-4	193214_s_at	4.8	nonessential intermediate filament protein that is coexpressed with the essential IF protein IFB-1	
T28F4.6		178783_at	4.8	contains similarity to Interpro domain IPR016024 (Armadillo-type fold)	
T25F10.3		186385_at	4.8	EGF-like, type 3;Delta/Serrate/lag-2 (DSL) protein;EGF-like, laminin;EGF;EGF-like region, conserved site	Y
ZK770.3	inx-12	180366_s_at	4.8	inx-12 (innexin=invertebrate connexin analogue) encodes a protein of the innexin family; innexins are the only known gap junction proteins in invertebrates	Y

Gene name	Locus	Affy Probe	Fold	Description	TM
Y66D12A.17	such-1	174877_at	4.8	such-1 encodes a component of the anaphase promoting complex/cyclosome (APC/C)	
W03D8.6	itx-1	188000_at	4.8	itx-1 encodes one of two Caspr orthologues found in the C. elegans genome; Caspr proteins belong to the Neurexin superfamily which mediate cell-cell contacts and in the formation of specialized membrane-domains in polarized epithelial and nerve cells	Y
F55D1.2		183246_at	4.7		
B0281.4		181853_at	4.7	Potassium channel, voltage dependent, Kv, tetramerisation;BTB/POZ fold;K+ channel tetramerisation domain	Y
W10D5.3	gei-17	188222_s_at	4.7	gei-17 encodes a protein containing a MIZ domain (Msx-interacting-zinc finger) that affects embryonic viability, vulval development, and body morphology; interacts with GEX-3 in yeast two-hybrid assays.	
F30F8.1		178648_s_at	4.7	contains similarity to Mus musculus Nuclear factor of activated T cells 5 (T cell transcription factorsNFAT5) (NF-AT5); SW:NFT5_MOUSE	
Y37E11AR.5	ugt-45	175194_at	4.7	UDP-glucoronosyl/UDP-glucosyl transferase family member	Y
F55A12.7	apm-1	193878_s_at	4.7	an ortholog of the mu1-II subunit of adaptor protein complex 1 (AP-1).	
C01B7.4	tag-117	189538_s_at	4.7	guanylate kinase	
T23B7.1	nspd-4	172486_x_at	4.6	Nematode Specific Peptide family, group D	
F20A1.6		181821_at	4.6		Y
F46F3.1	ceh-27	192317_at	4.6	ceh-27 encodes a homeodomain protein of the NK-2 class that contains Drosophila scarecrow and human NKX-2 (OMIM:606727)	
C03G6.17		185999_at	4.6	Acyl-CoA N-acyltransferase	
C24H12.5		187836_s_at	4.6	Immunoglobulin/major histocompatibility complex, conserved site	
D1086.3		177920_at	4.6	Protein of unknown function DUF19; Uncharacterised conserved protein UPF0376	Y
T19D7.5		180442_at	4.6	integral membrane protein	Y
Y42G9A.2		184890_at	4.5		Y
R08E5.2		189653_s_at	4.5	cysteine synthase	
F08G2.6	ins-37	188047_at	4.5	ins-37 encodes an insulin-like peptide.	Y
Y37H2A.6	fbxa-211	182392_at	4.5	a protein containing an F-box and an FTH/DUF38 motif	
F26D11.5	clec-216	185946_at	4.5	C-type lectin; C-type lectin fold	Y
C03E10.5	clec-223	182545_at	4.5	C-type lectin, Collagen triple helix repeat (20 copies), Proline-rich region	Y
F32H2.5	fasn-1	174796_at	4.5	fatty acid synthase, orthologous to human FASN (OMIM:600212)	
Y105C5B.6	srv-15	184967_at	4.5	srv-15, serpentine Receptor, class V	Y
C28C12.4		185803_at	4.5	contains similarity to Pfam domain PF02520 Domain of unknown function DUF148 contains similarity to Interpro domain IPR003677 (Protein of unknown function DUF148)	Y

Gene name	Locus	Affy Probe	Fold	Description	TM
C34G6.2	tyr-4	184158_at	4.4	Tyrosinase; Metridin-like ShK toxin	Y
C16B8.3		182754_at	4.4	Proline-rich region; Annexin, type VII	
T17H7.4	gei-16	174770_at	4.4	similar to the B20 antigen of the parasitic nematode Onchocerca volvulus; GEI-16 is required for ventral enclosure and elongation, larval development, and normal rates of postembryonic growth	
T10E9.3		183913_s_at	4.4	contains similarity to Pfam domain PF03351 DOMON	Y
Y38F2AL.1	nsy-4	177162_at	4.4	claudin homolog that may be required for normal cohesion of apical junctions in epithelia; Y38F2AL.1 is worm-specific, with obvious homologs only in C. elegans	Y
C27B7.5		190420_at	4.4	Zinc finger, CCHC class	
F36H5.10		174172_at	4.4	transmembrane protein	Y
W05E10.3	ceh-32	193576_at	4.4	Six/sine oculis-type homeodomain protein most closely related to the Six3/6 subfamily that contains Drosophila OPTIX and human SIX3 (holoprosencephaly 2)	
F56H6.2		177630_at	4.4	Protein of unknown function DUF268, Caenorhabditis species	Y
C01B7.5		180705_at	4.4	PDZ domain (Also known as DHR or GLGF)	
R03G5.2	sek-1	192392_at	4.4	SEK-1 has MAPKK activity and belongs to the MAPKK family; SEK-1 can activate both JNK-1 and PMK-1 in the yeast Hog pathway.	
K01C8.5	gei-14	188065_s_at	4.4	gei-14 encodes a novel protein that interacts with GEX-3 in yeast two-hybrid assays.	
C06A8.3		191204_s_at	4.4	Protein of unknown function DUF148;Domain of unknown function DUF148	Y
H08J19.1		182541_at	4.3	contains similarity to Homo sapiens formin-like 3 isoform 1	
T01D1.1		181722_s_at	4.3	conserved protein, contains double-stranded beta-helix domain, similar to IPR004313 (Acireductone dioxygenase, ARD), IPR014710 (RmlC-like jelly roll fold	
F38A5.3	lec-11	175705_s_at	4.3	Galectin, galactose-binding lectin; Concanavalin A-like lectin/glucanase	Y
B0353.1		187251_at	4.3	contains similarity to Synechocystis sp Serine/threonine-protein kinase C	
Y50D4B.2		176337_at	4.3	contains similarity to Homo sapiens Probable saccharopine dehydrogenase	
F21A9.2		189958_at	4.3	Zinc finger, C2H2-like	
F52H3.5		179402_at	4.3	TPR repeat containing protein	
C46H11.4	lfe-2	176895_s_at	4.3	inositol (1,4,5) triphosphate-3-kinase (IP3K); lfe-2 activity is required negative regulation of the LET-23 signaling pathway	
Y22D7AR.3		176340_at	4.3		
C47B2.1	fbxa-140	178679_at	4.3	protein containing an F-box and an FTH/DUF38 motif	Y

Gene name	Locus	Affy Probe	Fold	Description	TM
Y34D9A.10	vps-4	172130_at	4.3	AAA ATPase, core; MIT;Vps4 oligomerization, C-terminal; MIT (microtubule interacting and transport) domain	
F39B2.10	dnj-12	175394_at	4.2	contains a DnaJ domain, a prokaryotic heat shock protein	
Y46H3A.3	hsp-16.2	188282_at	4.2	heat shock protein (hsp-16.2)	
F26A1.3		189149_at	4.2	Protein kinase	
C27D6.4		188956_at	4.2	bZIP-1, Basic leucine zipper; cAMP response element binding (CREB) protein;Transcription factor Jun;Eukaryotic transcription factor, Skn-1-like, DNA-binding	
ZC239.2		181917_at	4.2	Polymerase delta-interacting protein PDIP1 and related proteins, contain BTB/POZ domain	
R07B1.4	gst-36	191221_at	4.2	glutathione S-transferase	
Y55B1AL.1		187111_at	4.2		
C33C12.4		185158_s_at	4.2	putative membrane protein	Y
F38A3.2	ram-2	194252_x_at	4.2	ram-2 encodes a cuticle collagen that interacts with unc-6 to affect ray cell migration, and interacts with unc-5 and unc-6 to affect embryonic viability	Y
C04F12.11		188825_s_at	4.2	transposon	
Y105E8A.16	rps-20	171977_x_at	4.1	rps-20 encodes a small ribosomal subunit S20 protein.	
F09E10.11	tts-1	174073_at	4.1	non-coding RNA transcript of unknown function	
F19B10.10		186728_s_at	4.1	Predicted E3 ubiquitin ligase	
C17G1.5		179127_s_at	4.1		Y
C02D4.2	ser-2	190313_at	4.1	tyramine 7-TM Domain receptor (GPCR)	Y
F53A9.6		172363_x_at	4.1	contains similarity to Interpro domains IPR002952 (Eggshell protein), IPR002395 (HMW kininogen)	
C30G12.6		187628_s_at	4.1	Armadillo-type fold	
F31A3.3		180056_at	4.1		
K09F6.6		181370_s_at	4.1	Small secreted protein with conserved cysteines	
F54E7.6		182110_at	4.0		Y
H25P19.1		175038_at	4.0		
Y39B6A.47	nhr-145	183498_s_at	4.0	nuclear hormone receptor	
C33A12.15	ttr-9	191296_at	4.0	Transthyretin-like family	Y
C48B4.2	rom-2	188662_at	4.0	contains similarity to Pfam domains PF01694 (Rhomboid family) , PF00036 (EF hand)	Y
Y57G11C.24	eps-8	193793_s_at	4.0	eps-8 is predicted to encode five protein isoforms with similarity to mouse epidermal growth factor receptor kinase substrate	
R07B7.10		191927_at	4.0	Mitochondrial substrate carrier;Mitochondrial carrier protein;Adenine nucleotide translocator 1	Y
F58G1.4	dct-18	177978_at	4.0	Endoplasmic reticulum, targeting sequence	Y
ZK675.1	ptc-1	192536_at	4.0	an ortholog of Drosophila PATCHED (PTC) and human PTCH, transmembrane protein	Y

Table S2. *fig-1* activity is required continuously for dye filling. Animals were cultivated on RNAi plates starting from different larval stages and were assayed for dye filling as young adults. In the case of L4 animals, this was 24 h of exposure. n = 50 for each.

	Normal Dye Filling (%)	
Larval stage	**Amphid**	**Phasmid**
L1 (empty vector)	100	100
L1	80	35
L2	85	43
L4	100	72

Supporting references and notes

1. S. Brenner, *Genetics* **77**, 71 (1974).
2. A. A. Beg, E. M. Jorgensen, *Nat. Neurosci.* **6**, 1145 (2003).
3. C. C. Mello, J. M. Kramer, D. Stinchcomb, V. Ambros, *EMBO J.* **10**, 3959 (1991).
4. M. D. Yandell, L. G. Edgar, W. B. Wood, *Proc. Natl. Acad. Sci. U.S.A.* **91**, 1381 (1994).
5. C. I. Bargmann, L. Avery, *Methods Cell Biol.* **48**, 225 (1995).
6. C. I. Bargmann, E. Hartwieg, H. R. Horvitz, *Cell* **74**, 515 (1993).
7. S. Ward, *Proc. Natl. Acad. Sci. U.S.A.* **70**, 817 (1973).
8. J. G. Culotti, R. L. Russell, *Genetics* **90**, 243 (1978).
9. W. S. Ryu, A. D. Samuel, *J. Neurosci.* **22**, 5727 (2002).
10. S. H. Chalasani *et al.*, *Nature* **450**, 63 (2007).
11. E. A. Lundquist, P. W. Reddien, E. Hartwieg, H. R. Horvitz, C. I. Bargmann, *Development* **128**, 4475 (2001).
12. M. Christensen *et al.*, *Neuron* **33**, 503 (2002).
13. R. M. Fox *et al.*, *BMC Genomics* **6**, 42 (2005).
14. R. S. Kamath *et al.*, *Nature* **421**, 231 (2003).
15. D. M. Miller, 3rd *et al.*, *Biotechniques* **26**, 914 (1999).
16. H. Fares, I. Greenwald, *Genetics* **159**, 133 (2001).
17. E. A. Perens, S. Shaham, *Dev. Cell* **8**, 893 (2005).
18. L. A. Perkins, E. M. Hedgecock, J. N. Thomson, J. G. Culotti, *Dev. Biol.* **117**, 456 (1986).
19. T. Bacaj, Y. Lu, S. Shaham, *Genetics* **178**, 989 (2008).
20. H. Qin, J. L. Rosenbaum, M. M. Barr, *Curr. Biol.* **11**, 457 (2001).
21. P. Sengupta, J. H. Chou, C. I. Bargmann, *Cell* **84**, 899 (1996).
22. H. Komatsu, I. Mori, J. S. Rhee, N. Akaike, Y. Ohshima, *Neuron* **17**, 707 (1996).